Research article

JHEP|Reports

A missense variant in human perilipin 2 (*PLIN2* Ser251Pro) reduces hepatic steatosis in mice

Eleonora Scorletti,[1,2,*] Yedidya Saiman,[3] Sookyoung Jeon,[4] Carolin V. Schneider,[5] Delfin G. Buyco,[6] Chelsea Lin,[7] Blanca E. Himes,[8] Clementina A. Mesaros,[9] Marijana Vujkovic,[1] Kate Townsend Creasy,[1] Emma E. Furth,[10] Jeffrey T. Billheimer,[2] Nicholas J. Hand,[1] David E. Kaplan,[11] Kyong-Mi Chang,[12,13] Philip S. Tsao,[14] Julie A. Lynch,[15] Joseph L. Dempsey,[16] Julia Harkin,[16] Susovon Bayen,[16] Donna Conlon,[17] Marie Guerraty,[17] Michael C. Phillips,[1] Daniel J. Rader,[1,2] Rotonya M. Carr[16]

[1]*Department of Genetics, Perelman School of Medicine, University of Pennsylvania, Philadelphia, PA, USA;* [2]*Division of Translational Medicine and Human Genetics, Department of Medicine, Perelman School of Medicine at the University of Pennsylvania, Philadelphia, PA, USA;* [3]*Department of Hepatology, Lewis Katz School of Medicine, Temple University, Philadelphia, PA, USA;* [4]*Department of Food Science and Nutrition, Hallym University, Chuncheon, Gangwon-do, Republic of Korea;* [5]*Department of Medicine III, Gastroenterology, Metabolic Diseases and Intensive Care, University Hospital RWTH Aachen, Aachen, Germany;* [6]*Department of Biomedical Engineering, Northwestern University, Evanston, IL, USA;* [7]*School of Medicine, Oregon Health & Science University, Portland, OR, USA;* [8]*Department of Biostatistics, Epidemiology and Informatics, Perelman School of Medicine, University of Pennsylvania, Philadelphia, PA, USA;* [9]*Department of Systems Pharmacology and Translational Therapeutics (SPATT) University of Pennsylvania, Philadelphia, PA, USA;* [10]*Department of Pathology and Laboratory Medicine, Perelman School of Medicine, University of Pennsylvania, Philadelphia, PA, USA;* [11]*Division of Gastroenterology and Hepatology, Perelman School of Medicine, University of Pennsylvania, Philadelphia, PA, USA;* [12]*Corporal Michael J. Crescenz VA Medical Center, Philadelphia, PA, USA;* [13]*Perelman School of Medicine, University of Pennsylvania, Philadelphia, PSA, USA;* [14]*Precision Medicine, VA Palo Alto Health Care System, Palo Alto, CA, USA;* [15]*VA Informatics & Computing Infrastructure, VA Salt Lake City Utah & University of Utah, School of Medicine, Salt Lake City, UT, USA;* [16]*Division of Gastroenterology, Department of Medicine, School of Medicine, University of Washington, Seattle, WA, USA;* [17]*Division of Cardiovascular Medicine, Department of Medicine, University of Pennsylvania, PA, USA*

JHEP Reports **2024.** https://doi.org/10.1016/j.jhepr.2023.100902

Background & Aims: Non-alcoholic fatty liver disease (NAFLD) is characterised by the accumulation of lipid droplets (LDs) within hepatocytes. Perilipin 2 (PLIN2) is the most abundant protein in hepatic LDs and its expression correlates with intracellular lipid accumulation. A recently discovered *PLIN2* coding variant, Ser251Pro (rs35568725), was found to promote the accumulation of small LDs in embryonic kidney cells. In this study, we investigate the role of *PLIN2*-Ser251Pro (PLIN2-Pro251) on hepatic LD metabolism *in vivo* and research the metabolic phenotypes associated with this variant in humans.
Methods: For our animal model, we used *Plin2* knockout mice in which we expressed either human *PLIN2-Pro251* (Pro251 mice) or wild-type human *PLIN2-Ser251* (Ser251 mice) in a hepatocyte-specific manner. We fed both cohorts a lipogenic high-fat, high-cholesterol, high-fructose diet for 12 weeks.
Results: Pro251 mice were associated with reduced liver triglycerides (TGs) and had lower mRNA expression of fatty acid synthase and diacylglycerol O-acyltransferase-2 compared with Ser251 mice. Moreover, Pro251 mice had a reduction of polyunsaturated fatty acids-TGs and reduced expression of epoxygenase genes. For our human study, we analysed the Penn Medicine BioBank, the Million Veteran Program, and UK Biobank. Across these databases, the minor allele frequency of *PLIN2-Pro251* was approximately 5%. There was no association with the clinical diagnosis of NAFLD, however, there was a trend toward reduced liver fat in *PLIN2-Pro251* carriers by MRI-spectroscopy in UK Biobank subjects.
Conclusions: In mice lacking endogenous *Plin2*, expression of human *PLIN2-Pro251* attenuated high-fat, high-fructose, high-cholesterol, diet-induced hepatic steatosis compared with human wild-type *PLIN2-Ser251*. Moreover, Pro251 mice had lower polyunsaturated fatty acids-TGs and epoxygenase genes expression, suggesting less liver oxidative stress. In humans, *PLIN2-Pro251* is not associated with NAFLD.
Impact and Implications: Lipid droplet accumulation in hepatocytes is the distinctive characteristic of non-alcoholic fatty liver disease. Perilipin 2 (PLIN2) is the most abundant protein in hepatic lipid droplets; however, little is known on the role of a specific polymorphism *PLIN2-Pro251* on hepatic lipid droplet metabolism. *PLIN2-Pro251* attenuates liver triglycerides accumulation after a high-fat-high-glucose-diet. *PLIN2-Pro251* may be a novel lipid droplet protein target for the treatment of liver steatosis.

Keywords: NAFLD; Lipid droplets; Perilipin; DGAT2; triglycerides.
Received 21 December 2022; received in revised form 1 August 2023; accepted 24 August 2023; available online 11 October 2023
* Corresponding author. Address: Perelman School of Medicine at The University of Pennsylvania, Division of Translational Medicine and Human Genetics, Smilow Center for Translational Research, Room 11-130-3, 3400 Civic Center Blvd., Philadelphia, PA 19104, USA.
E-mail address: eleonora.scorletti@pennmedicine.upenn.edu (E. Scorletti).

Introduction

Non-alcoholic fatty liver disease (NAFLD) is a chronic and heterogenous liver condition characterised by the presence of lipid droplets (LDs) in more than 5% of the hepatocytes.[1] NAFLD affects approximately 25% of the adult population worldwide.[2] This condition can gradually progress into non-alcoholic steatohepatitis (NASH), liver fibrosis, cirrhosis, and hepatocellular carcinoma.[3] There is currently no effective treatment for NAFLD, and as a result, this condition has become one of the most common causes of cirrhosis, liver disease-related mortality, and liver transplantation.[4] As the progression of NAFLD is associated with the accumulation of hepatic LDs and dysregulated glucose metabolism, understanding the specific mechanisms underlying LD accumulation is key to develop novel diagnostic and therapeutic strategies.[3]

Triglycerides (TGs) that accumulate in hepatocytes are stored in LDs. LDs are active, storage organelles with a unique architecture consisting of a hydrophobic core of neutral lipids (predominantly cholesterol esters and TGs) enveloped in a phospholipid monolayer. In this monolayer lie heterogeneous proteins and enzymes responsible for neutral lipid synthesis and metabolism.[5] Perilipin 2 (PLIN2) is the most abundant hepatic protein in the LD phospholipid monolayer.[6,7] PLIN2 plays an important role in the formation and stability of LDs and lipophagy,[7–11] and is associated with increased long-chain ceramides[12] that impair insulin signalling.[9,11,13]

Previous studies showed that gene variants affecting liver TG metabolism were associated with a high risk of developing hepatocellular carcinoma irrespective of severe fibrosis.[14,15]

Recently, a human *PLIN2* missense variant characterised by a serine-to-proline substitution at position 251 (Ser251Pro; rs35568725) was shown to have an impact on LD structure and lipid metabolism. The *PLIN2*-Ser251Pro (*PLIN2-Pro251*) variant was found to promote LD accumulation in a range of cell types, including macrophages, human embryonic kidney 293 cells, and hepatic cells (HuH7 cells).[16,17] By contrast, there are conflicting results regarding the effect of *PLIN2-Pro251* on cellular TG accumulation.[16,17] In humans, the *PLIN2-Pro251* variant has been associated with reduced plasma levels of TGs and VLDLs.[16] However, the molecular role of *PLIN2-Pro251* in LD metabolism is not well understood.

In the current study, we developed an experimental mouse model to investigate the biologic role of human *PLIN2-Pro251* on hepatic lipid metabolism. We found that the *PLIN2-Pro251* variant reduced liver TGs and LD accumulation compared to the wild-type human *PLIN2-Ser251*. Concurrently, we analysed the Penn Medicine BioBank (PMBB), the Million Veteran Program (MVP) and UK Biobank (UKB), three large and well-validated databases, to determine the metabolic phenotypes associated with *PLIN2-Pro251*. Our analyses revealed that this variant is not associated with NAFLD and data from the UKB also showed that *PLIN2-Pro251* carriers have reduced liver fat compared with non-carriers. Our results offer insights into the role of *PLIN2-Pro251* in hepatocellular LD homeostasis and provide a basis for future investigations.

Materials and methods

Animal model

For our study, we used 8–10-week-old male *Plin2* KO-mice (Supplementary material).[9] (Male mice were used to interrogate the effect of Pro251 on lipid droplet biology, as female mice were relatively protected from steatosis in our pilot study of 12 weeks of high-fat, high-fructose, high-cholesterol [FFC] feeding.) Mice were fed with chow diet until they were 8 weeks old. Thereafter, we administered a retro-orbital injection of adeno-associated virus utilising a thyroxine-binding globulin promoter to direct the expression of either the *PLIN2-Pro251* polymorphism (Pro251 mice) or the wild-type *PLN2-Ser251* (Ser251 mice) in the liver (Fig. S1A–D).

All injected mice were divided into two dietary groups: the first group (FFC group) was given 12 weeks of *ad libitum* access to an FFC diet (40% kcal fat, 20% kcal fructose, 2% cholesterol); the second group (Chow group) was given 12 weeks *ad libitum* access to a chow diet (Fig. S1E).[18]

Biochemical and lipidomic analysis

Plasma samples for biochemical assays were obtained by centrifuging blood in a lithium heparin tube at 2,000 × *g* at 4 °C for 10 min. Liver samples were prepared by adding 6 μl 2:1 ethanol (EtOH):30% potassium hydroxide solution per mg of liver tissue, vortexing, then incubating in a 60 °C water bath overnight. Subsequently, 1.08 volumes of 1 $MgCl_2$ were added to the liver digest, before it was vortexed to a milky consistency, and placed on ice for 10 min. The liver digest was then centrifuged at 18,000 × *g* at room temperature for 30 min, and the resulting supernatant was used for biochemical assays.

Plasma alanine aminotransferase (ALT) activity was measured using a Stanbio ALT/SGPT Liqui-UV Test kit (EKF Diagnostics, TX, USA). Plasma and liver TG levels were measured using a Stanbio Triglycerides LiquiColor Test Mono (EKF Diagnostics, TX, USA). Plasma levels of non-esterified fatty acid (NEFA) were measured using a Wako HR Series NEFA-HR 2 test kit (Fujifilm, Japan). All biochemical assays were analysed using Infinite 200 PRO plate reader (Tecan Trading AG, Switzerland). Fasting blood glucose was measured using the Accu-Chek Nano Glucose Meter (Roche Diabetes Care, Inc., New York, NY, USA).

To estimate hepatic VLDL production, a kinetic experiment was performed. Mice were fasted for 4 h (from 07:00 to 11:00) then injected with 1 g/kg poloxamer 407 (Sigma-Aldrich, St. Louis, MO, USA) that blocks the lipolysis of TGs. Tail vein blood was collected at time 0 and 1, 2, and 4 h after injection, measuring TGs by colorimetric assay and thereby enabling estimation of VLDL secretion rate.

Lipidomics

Tissue preparation for lipids extraction

Sections of approximately 10 mg of frozen tissues were cut on a tile kept in dry ice with a new blade kept in dry ice. The tissue was added to a microcentrifuge tube with 0.6 ml 80% methanol (MeOH) and 20 μl on internal standard mix (1:1, SPLASH® LIPIDOMIX #330707 and Ceramide/Sphingoid Internal Standard Mixture I #LM6002, both from Avanti Polar Lipids, Alablaster, AL, USA).

Liquid chromatography-high resolution mass spectrometry for lipids

Metabolites were separated using an Ascentis Express C18, 2.1 × 150 mm 2.7 μm column (Sigma-Aldrich) on an UltiMate 3000 HPLC system. The metabolites were eluted on a 0.4 m/min flow-rate gradient using Solvent A (4:6 v/v water:acetonitrile, 0.1% formic acid, 10 mM ammonium formate) and Solvent B (1:9 v/v acetonitrile:isopropanol, 0.1% formic acid, 10 mM ammonium formate). The gradient was as follows: 10% B at 0 min, 10% B at

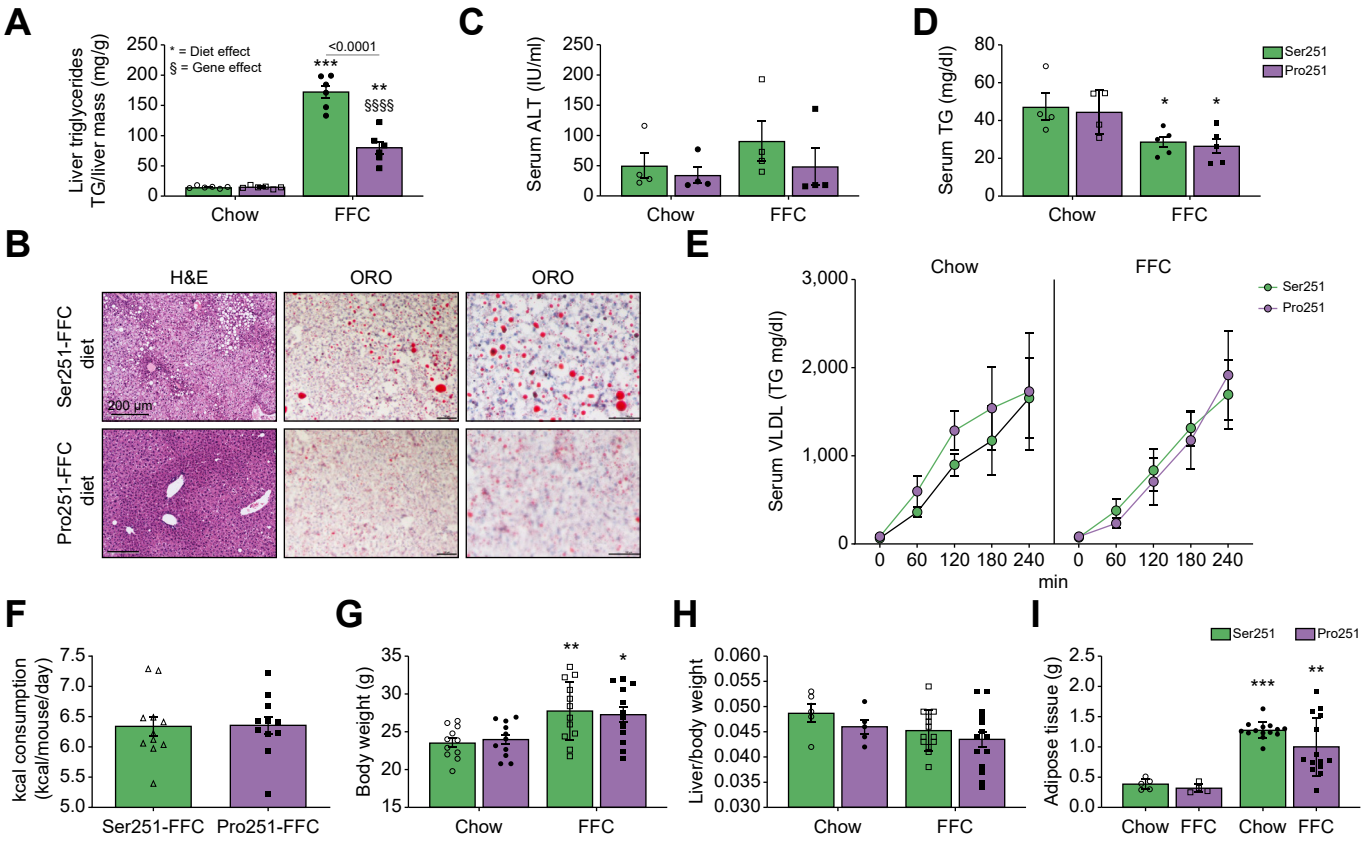

Fig. 1. Impact of Pro251 on hepatic and metabolic parameters in mice after 12-week FFC diet. Hepatic TG levels (A), representative histologic images of H&E-stained and Oil Red O stained (B), hepatic ALT (C), serum TG levels (D), serum VLDL (E), calories consumed (F), body weights (G), liver/body weight ratio (H), adipose weight (I). Statistical analyses were performed using a two-tailed unpaired *t*-test or one-way ANOVA with Tukey's *post-hoc* test. *Statistical difference between diets, *p <0.05; **p <0.005; ***p <0.0005; ****p <0.0001. §Statistical difference between genotypes, §p <0.05; §§p <0.005; §§§p <0.0005; §§§§p <0.0001. ALT, alanine aminotransferase; FFC, high-fat, high-fructose, high-cholesterol; TG, triglyceride; VLDL, very low density lipoprotein.

1 min, 40% B at 4 min, 75% B at 12 min, 99% B at 21 min, 99% B at 24 min, 10% B at 24.5 min, 10% at 30 min. Separations were performed at 55 °C.

For the lipidomic and ceramide analyses see the Supplementary material.

Histology

Dissected liver samples were placed in a cartridge, fixed in 10% buffered formalin overnight, transferred to 70% EtOH, and paraffin embedded. Paraffin sections were stained with H&E. To visualise lipid deposition, liver sections frozen in cryoprotectant media were stained with Oil Red O. Sectioning and staining of the liver were performed by the Molecular Pathology and Imaging Core at the University of Pennsylvania. Slides were visualised under a bright field with Nikon 80i microscope (Nikon Instruments, Melville, NY, USA) and interpreted by a liver pathologist (EEF). Images were captured with a Nikon DS-Qi1MC camera (Nikon Instruments).

Western blot

Tissue protein lysates were prepared by homogenising liver, adipose, or muscle tissue in a RIPA buffer (50 mM Tris [pH 8.0], 150 mM NaCl, 5 mM EDTA, 1% v/v NP-40, 0.5% w/v sodium deoxycholate, 0.1% v/v SDS, 50 mM sodium fluoride) containing cOmplete Protease Inhibitor tablets and PhosStop phosphatase inhibitor tablets (Roche Diagnostics, Germany). Protein concentrations were determined using a Pierce BCA protein assay kit (Thermo-Fisher Scientific). Proteins were then resolved on a NuPAGE 4–12% Bis-Tris gel (Invitrogen, CA, USA) by electrophoresis, and transferred onto a nitrocellulose membrane by electroblotting. Blots were analysed using ImageJ software (NIH). Data were normalised to glyceraldehyde 3-phosphate dehydrogenase protein levels.

Quantitative PCR

Liver tissue samples stored in RNAlater solution (Invitrogen, Lithuania) were solubilised using a Bio-Gen PRO 200 homogeniser (PRO Scientific, CT, USA). mRNA was extracted from the homogenate using a PureLINK RNA Mini Kit (Invitrogen, CA, USA). The mRNA samples were treated with Amplification Grade DNase I (Invitrogen, CA, USA), then MultiScribe reverse transcriptase (Applied Biosystems, CA) to produce cDNA. Quantitative real-time PCR (qPCR) was performed with the cDNA on a StepOnePlus PCR system (Applied Biosystems, CA, USA) or Taqman 7900 (Thermo-Fisher Scientific) using gene-specific primers and SYBR Select Master Mix (Applied Biosystems, Lithuania). Data were normalised to mRNA levels of ribosomal protein, large, P0 (36b4) reference gene.

Glucose and insulin tolerance test

For glucose tolerance tests (GTTs), mice were fasted for 6 h and then intraperitoneally injected with PBS supplemented with 20% glucose at a dosage of 10 ml/kg body weight. Blood glucose levels were measured at time 0 and 15, 30, 60, 120, and 180 min after injection with an ACCU-CHEK Inform II glucometer (Roche Diabetes Care, IN, USA). For the insulin tolerance test (ITT), animals were fasted for 5 h before 0.75 U/kg of human insulin was intraperitoneally administered. Tail blood glucose was measured at time 0 and 15, 30, 60, and 90 min after injection with a glucometer (Lifescan, Inc., Milipitas, CA, USA). Mice were allowed to recover and resume their diets after completion of these tests.

Metabolic monitoring

Mice were individually placed in the Oxymax Lab Animal Monitoring System (Columbus Instruments, Columbus, OH, USA). Following a 24-h acclimation period, oxygen consumption, carbon dioxide production, and locomotor activity were determined. The respiratory exchange ratio (RER) was calculated by dividing the volume of carbon dioxide produced by the volume of oxygen consumed (VCO_2/VO_2). Whole body fat and lean mass determinations were performed using the Eco-MRI-100 system (Echo MRI; Houston, TX, USA).

RNA-seq

mRNA samples for RNA-seq analysis were prepared from liver tissue homogenates using a PureLINK RNA Mini Kit (Invitrogen, CA, USA). Libraries were prepared by the Next Generation Sequencing Core at the University of Pennsylvania. Total RNA quantity and quality were assayed with an Agilent 2100 Bioanalyzer instrument using the RNA 6000 Nano Kit (Agilent Technologies). Libraries were prepared at Next Generation Sequencing Core at the University of Pennsylvania using TruSeq Stranded mRNA HT Sample Prep Kit (Illumina) as per standard protocol in the kit's sample prep guide. Libraries were assayed for size using the DNA 1000 kit of an Agilent 2100 Bioanalyzer (Agilent Technologies) and quantified using the KAPA Library Quantification Kit for Illumina platforms (KAPABiosystems). The 100-bp single-read sequencing of multiplexed samples was performed on an Illumina HiSeq 4000 sequencer. Illumina's bcl2fastq version 2.20.0.422 software was used to convert bcl to fastq files.

The Penn Medicine Biobank

The PMBB is an institutional resource of the University of Pennsylvania Health System. This database includes DNA, blood, and tissue samples from over 60,000 patients. Samples were obtained under a single umbrella Institutional Review Board protocol that permits DNA genotyping and sequencing, biomarker assays, access to electronic health record (EHR) phenotype data, and permission to recontact. PMBB participants were genotyped using the Illumina Global Screening Array v.2.0 and further imputed using the TOPMed Imputation Server. For the phenome-wide association study (PheWAS), ICD-9 and ICD-10 codes were used to assign traits to each patient according to their records, and a genome-wide association study for each was run using the imputed genome-wide genetic data. Subsequently, the results for rs35568725 were retrieved to determine its association with clinical phenotypes. For our study, we screened the genome-wide genotype data for over 20,000 White and Black participants.

Million Veteran Program

The US Department of Veterans Affairs (VA) provides care to approximately nine million veterans. The MVP is a VA database of genomic and phenotypic information.[19,20] Launched in 2011 and supported by the Veterans Health Administration Office of Research and Development in the United States, the MVP largely comprises White, Black, and Hispanic male veteran participants and contains both clinical and genetic data. Clinical data were prospectively collected and combined with prior health record data from the VA EHR, and the VA Corporate Data Warehouse. The association of cardiometabolic traits for *PLIN2-Pro251* among MVP participants was tested under an additive logistic model and was corrected for age, sex, and the first 10 ethnicity-specific principal components. The present study was approved by the VA Central Institutional Review Board and by the Corporal Michael J. Crescenz VA Medical Center and by the University of Pennsylvania Institutional Review Board.

The United Kingdom Biobank

The UKB is a population-based cohort study, which recruited 502,505 UK volunteers between 2006 and 2010 (age range between 37 and 73 years). Genome-wide genotyping was performed using the UKB Axiom Array and additional imputation was performed using the TOPMed reference panel. The UKB was approved by the Northwest Multi-Center Research Ethics Committee. Details of the methods, data availability, and access procedures for UKB are publicly disclosed on its website (http://www.ukbiobank.ac.uk). A total of 1,419 EHR-derived broad PheWAS codes were available for approximately 400,000 White British individuals. For liver fat analysis and adipose tissue analysis we used UKB MRI-derived phenotypes. For our study, association analyses were performed using the logistic regression test implemented in plink, including age, sex, and 10 ancestry-informative principal components as covariates.

Data analysis

Statistical analyses for the *in vivo* model were performed using GraphPad Prism 8.2 (GraphPad, San Diego, CA, USA). All data were presented as mean ± standard error of measurement (SEM). Statistical analysis was performed using either a *t* test or one-way ANOVA with Tukey's multiple comparisons test. To test for any independent associations linear or logistic regressions were performed. Statistical significance was determined at $p < 0.05$. The following programs were used to analyse our collected data: R version 4.0.2 (R Foundation for Statistical Computing; Vienna, Austria), SPSS Statistics version 26 (IBM; Armonk, NY, USA) and Prism version 8 (GraphPad, La Jolla, CA, USA). We calculated the Bonferroni corrected/adjusted *p* value, by dividing the original α-value (0.05) by the number of analyses on the dependent variable.

Results

PLIN2-Pro251 expression attenuates FFC-induced hepatic steatosis compared with PLIN2-Ser251

After 12 weeks of the FFC diet, we found that Pro251 mice had a significantly lower hepatic TG level compared with Ser251 mice (Fig. 1A and B). In addition, the liver histology showed a shift in LD organisation with increasing microvesicular patterns in Pro251 mice compared with Ser251, without evidence of inflammation or fibrosis in either genotype (Fig. 1B and Fig. S1E).

Moreover, FFC-fed Pro251 and Ser251 mice showed similar liver ALT levels, serum TG levels, and hepatic VLDL-TG secretion (Fig. 1C–E). Pro251 and Ser251 mice also had similar caloric consumption, increase in body weight, liver to body weight ratio, and adipose tissue weight (Fig. 1F–I).

PLIN2-Pro251 has a role in liver lipid remodelling

Given the changes observed with overall hepatic TG content and reduction in steatosis in Pro251 mice, we quantified the specific lipid species that contribute to liver LD composition. We performed a targeted shotgun comparison of hepatic lipids obtained from liver lysates of Pro251 and Ser251 mice. The lipidomic analysis demonstrated that Pro251 mice had a decrease in total hepatic TG species compared with Ser251 mice (Fig. 2A), confirming our biochemical measurements. In addition, we found a trend towards a reduction of total hepatic diacylglycerols (DGs) in Pro251 compared with Ser251 mice (Fig. 2B). We did not find any difference in total hepatic levels of cholesterol esters, lysophosphatidylcholine, phosphatidylethanolamine, phosphatidylcholine, and sphingomyelin in both genotypes (Fig. 2C–G); however, we found a trend towards increase in acyl-CoA (Fig. 2H).

A detailed analysis of the lipid species demonstrated a reduction in the quantity of polyunsaturated-fatty-acids-TG (PUFA-TG) in Pro251 mice (Fig. 3A and B and Table S1). In both diets, Pro251 mice had a significant reduction in TG (18:1_18:1_22:3), TG (18:0_22:6_22:6), TG (20:5_17:1_18:2), TG (18:2_17:1_18:2), TG (16:0_14:0_18:1) TG (18:0_16:0_16:0), and TG (18:1_14:0_14:0) (Fig. 3B and Table S1). Interestingly, we

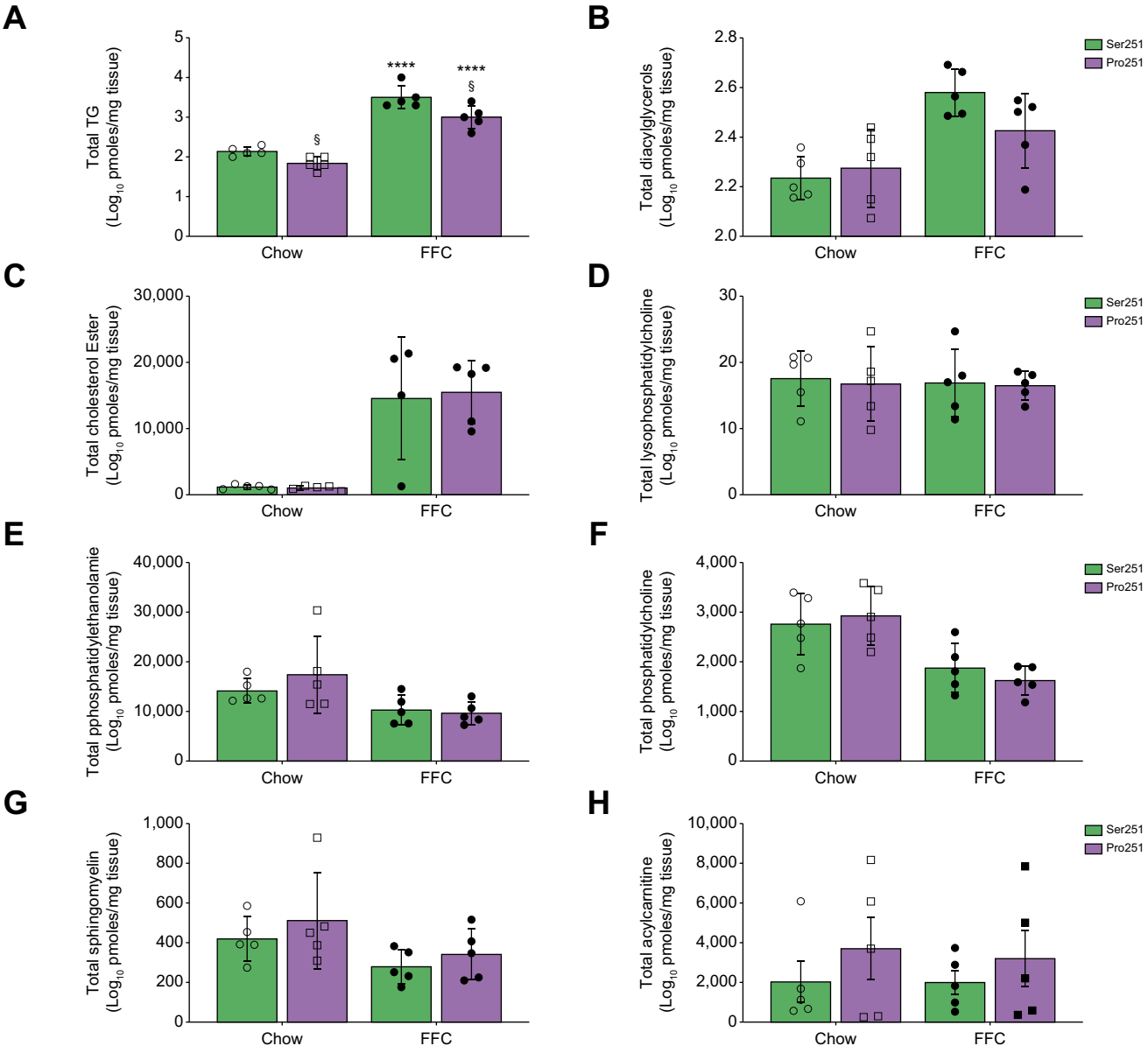

Fig. 2. Liver lipidomic analysis. Total triglycerides (TG) (A), diacylglycerols (DG) (B), total cholesterol ester (C), total lysophosphatidilcholine (D), total phosphatidylethanolamine (E), total phosphatidylcholine (F), total sphingomyelin (G) and acylcarnitine (H). Statistical analyses were performed using a two-tailed unpaired *t*-test or one-way ANOVA with Tukey's *post-hoc* test. *Statistical difference between diets, *p <0.05; **p <0.005; ***p <0.0005; ****p <0.0001. §Statistical difference between genotypes, §p <0.05; §§p <0.005; §§§p <0.0005; §§§§p <0.0001. FFC, high-fat, high-fructose, high-cholesterol.

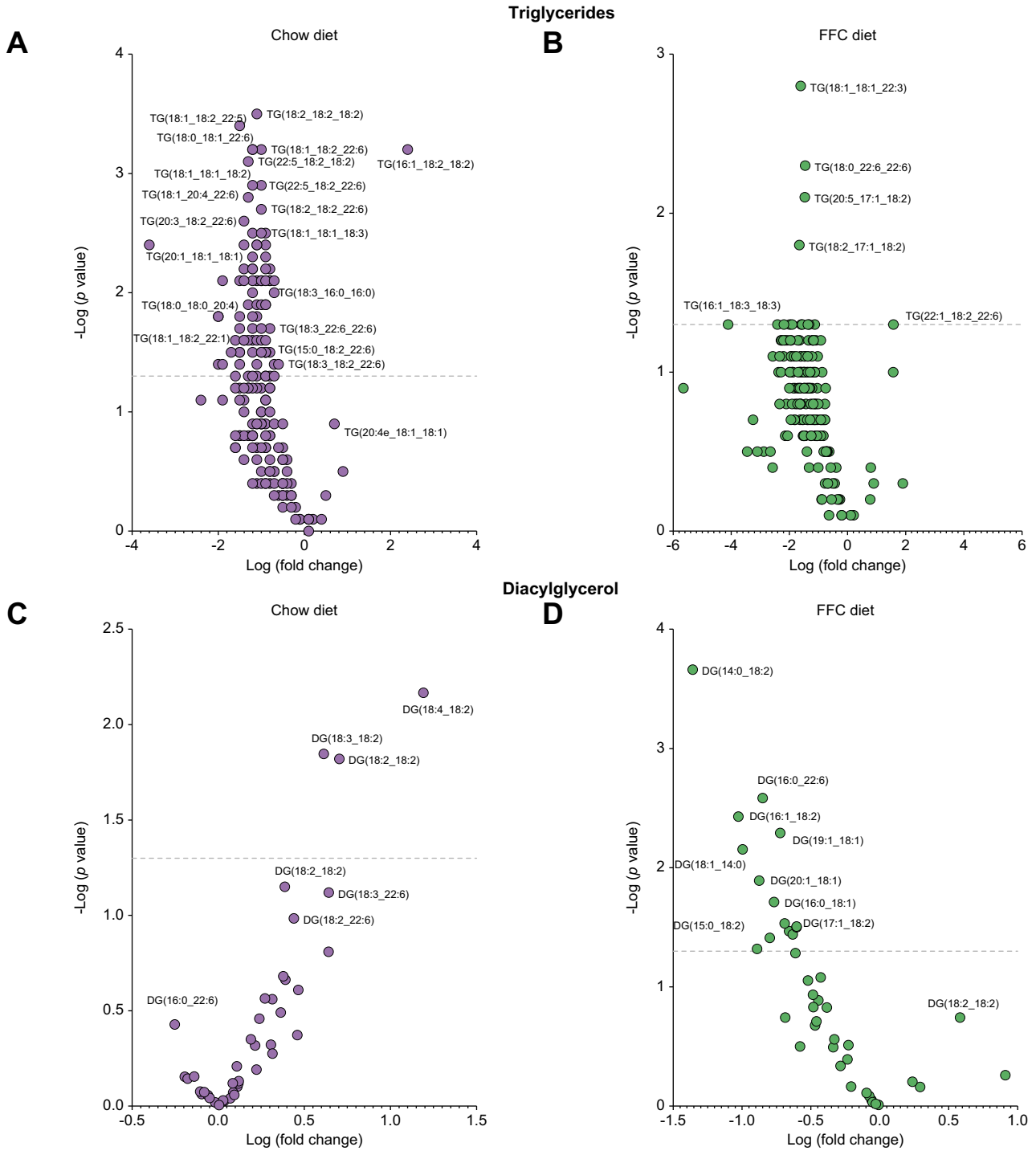

Fig. 3. Volcano plot showing the log-fold changes of lipids in Pro251 mice. Liver triglycerides in chow diet (A) and FFC diet (B); liver diacylglycerols (C) and (D). The line marks the Bonferroni significant cut-off. FFC, high-fat, high-fructose, high-cholesterol; TG, triglyceride.

found that in the Chow group, there was an increase in PUFA-DG in Pro251 mice; whereas, in the FFC group, Pro251 mice had a reduction in DG containing saturated and monounsaturated fatty acids compared with Ser251 mice (Fig. 3C and D). With regard to other lipids, Pro251 mice fed an FFC diet also had a trend towards increase in PC containing α-linolenic acid PC (18:3e_18:0) and lower (albeit non statistically significant) levels of PE containing docosapentaenoic acid PE (18:1_22:5) and linoleic acid (18:1_18:2) compared with Ser251.

Having previously established that ceramides are also present in the LD fraction,[12,21] we analysed the distribution of several serum and hepatic sphingolipids in Pro251 and Ser251 mice using mass spectrometry (Fig. S2A–H). The overall patterns of serum and hepatic sphingolipids – both upstream (*i.e.* dihydrosphingosine) and downstream (*i.e.* sphingosine) in the ceramide metabolic pathway – were similar in both genotypes. In the FFC-diet group, Pro251 mice had lower levels of C20 compared with Ser251 mice. These observations are important

as higher C20 ceramide is positively associated with cardiometabolic risk.[22]

Expression of PLIN2-Pro251 downregulates expression of genes associated with fatty acid synthesis and epoxygenase P450 pathway

To gain insight into the molecular mechanisms of *PLIN2-Pro251*, we investigated the effect of this variant on hepatic lipids. First, we performed RNA-seq in the liver samples of our mice in both diet groups. The principal component analysis showed a clear separation between both FFC and Chow groups and slight separation between both genotypes (Pro251 and Ser251) in the FFC group (Fig. 4A). With regard to the differentially expressed genes (DEGs), we found 46 genes that were significantly downregulated and 30 genes that were significantly upregulated in the Pro251 mice compared with the Ser251 mice. Among downregulated genes, gene enrichment analysis identified several significantly altered metabolic pathways, including epoxygenase P450 pathway (*Cyp2b13*, *Cyp2b9*, *Cyp2a22*, and *Cyp3a59*), fatty acid metabolism (*Mogat1*, *Fasn*, and *Hsd17b12*), and glutathione metabolism pathway (*Gstm3* and *Gstt1*). With regard to the upregulated genes, gene enrichment analysis showed altered pathways involved in immune signalling and responses (*Ikbkg*, *Junb*, *Egr1*, *Fos*, and *Fosb*) and a gene involved in the fatty acyl-CoA synthesis that controls mitochondrial respiratory capacity (*Acsbg1*) (Fig. 4B and C).

We validated these findings using qPCR of representative genes. In the FFC group, hepatic mRNA levels of lipogenic genes were upregulated in both Pro251 and Ser251 mice. However, compared with Ser251 mice, fatty acid synthase (*Fasn*) and diacylglycerol O-acyltransferase 2 (*Dgat2*) expression were significantly downregulated in Pro251 mice, indicating that they had less fatty acid synthesis and less conversion of diacylglycerol and fatty acyl-CoA to TGs (Fig. 5A and B). However, we did not observe any differences in DGAT2 protein expression between Ser251 and Pro251 mice (data not shown). We did not find significant changes in mRNA expression of peroxisome proliferator-activated receptor alpha or gamma in both genotypes (Fig. 5C) or in genes associated with inflammation, autophagy, cellular stress, or glucose metabolism (Fig. 5D–F). Moreover, there was no significant difference in *Plin1*, *Plin3* mRNA, and protein expression between Pro251 and Ser251 mice (Fig. 5G and Fig. S3A–C).

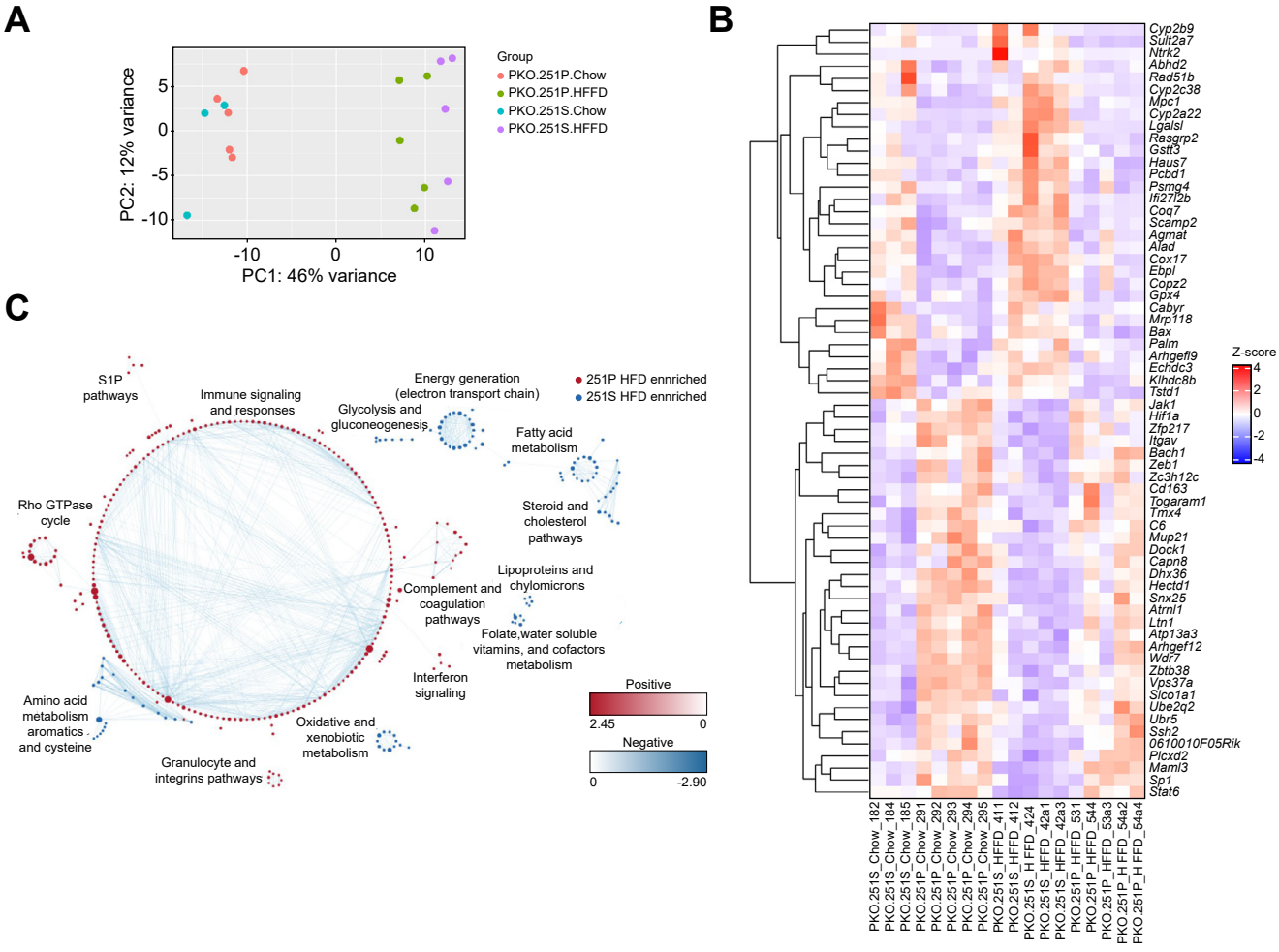

Fig. 4. Liver differentially expressed genes in Pro251 and Ser251. Principal component analysis showing a clear separation between the FFC and chow group and slight separation between both genotypes (Pro251 and Ser251) in the FFC group (A). Each dot represents data from individual mice (A); a heatmap depicts 36 DEGs that were significantly changed in the Pro251 compared with Ser251 in the FFC group (B); 13 enrichment pathways identified using GSEA and Cytoscape (C). DEGs, differentially expressed genes; FFC, high-fat, high-fructose, high-cholesterol.

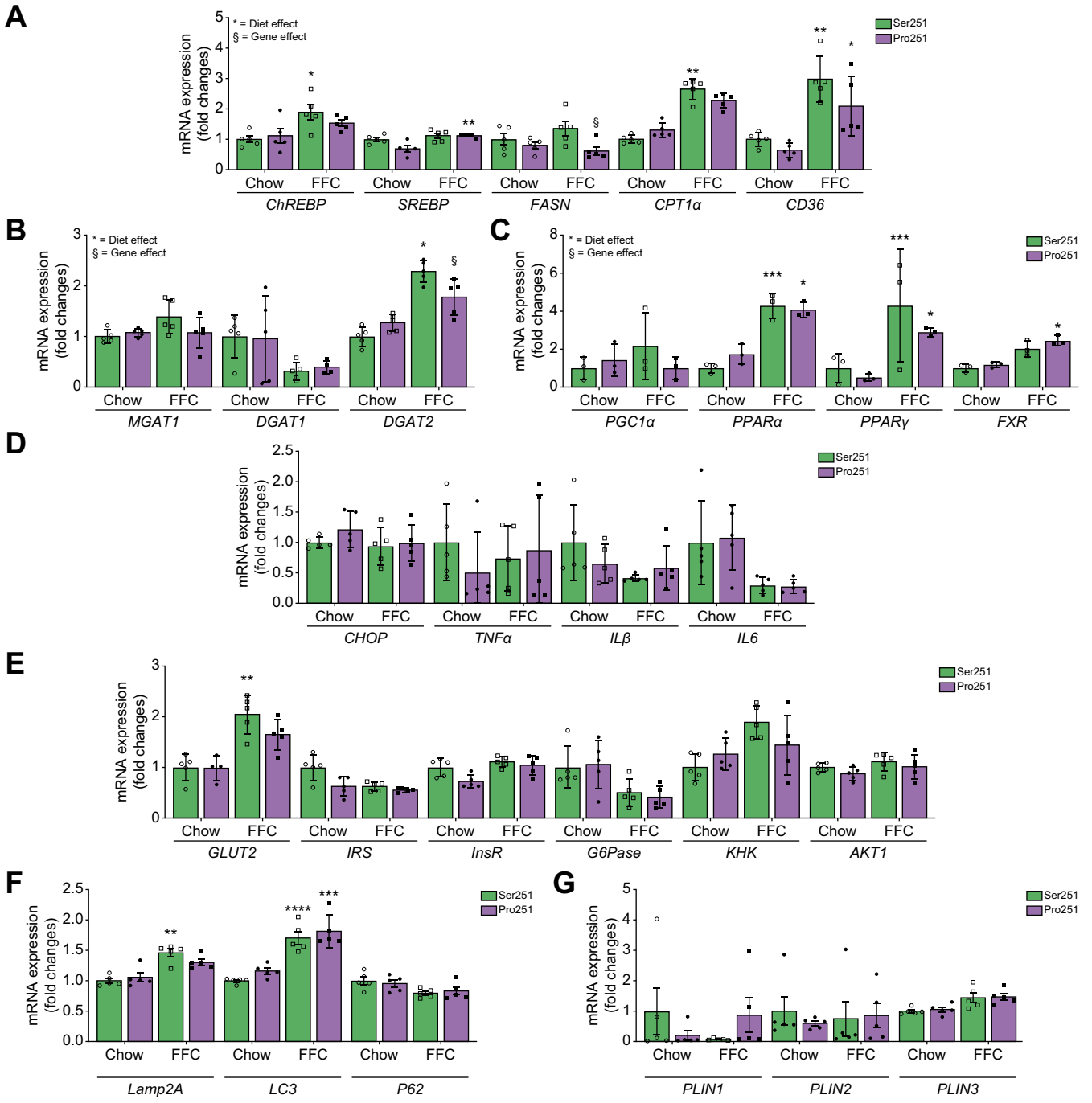

Fig. 5. *De novo* lipogenesis gene expression measured by qPCR mice on chow and FFC diets. (A) lipogenesis gene expression measured by qPCR in mice on chow and FFC diets (B), MGAT, DGAT1, DGAT2 gene expression measured by qPCR in mice on chow and FFC diets (C), inflammatory response gene expression measured by qPCR in mice on chow and FFC diets (D), glucose metabolism genes expression measured by qPCR in mice on chow and FFC diets (E), autophagy gene expression measured by qPCR in mice on chow and FFC diets (F), PLIN1, PLIN2, and PLIN3 gene expression by qPCR in mice on chow and FFC diets (G). Statistical analyses were performed using a two-tailed unpaired *t*-test or one-way ANOVA with Tukey's *post-hoc* test. **p* <0.05; ***p* <0.005; ****p* <0.0005; *****p* <0.0001. §Statistical difference between genotypes, §*p* <0.05; §§*p* <0.005; §§§*p* <0.0005; §§§§*p* <0.0001. DGAT, diacylglycerol acyltransferase; FFC, high-fat, high-fructose, high-cholesterol; MGAT, monoacylglycerol acyltransferase; PLIN, perilipin; qPCR, quantitative real-time PCR.

PLIN2-Pro251 has no effect on glucose tolerance or insulin sensitivity

To determine the effect of *PLIN 2-Pro251* on insulin sensitivity, we performed an intraperitoneal GTT and ITT. We found no differences in fasting blood glucose (Fig. S4A), GTT or ITT (Fig. S4B and C) between the genotypes. In addition, we did not find differences in serum NEFA (a surrogate measure of adipose tissue insulin sensitivity) between the two genotypes (Fig. S4D).

PLIN2-Pro251 expression increases energy expenditure

To evaluate the effect of the *PLIN2-Pro251* on metabolic phenotypes, we measured energy expenditure with indirect

calorimetry (Fig. 6). Throughout the day, Pro251 mice had increased O_2 consumption, CO_2 production and energy expenditure compared with Ser251 mice (Fig. 6A–C). We also measured the RER which equals VCO_2/VO_2). RER is an index of fuel oxidation: a RER value of 0.7 indicates fat oxidation, whereas a value of 1 indicates carbohydrate oxidation. Pro251 mice had significantly reduced RER values compared with Ser251 mice, in the dark period. Notably, in Pro251 mice, RER levels were approximately 0.8, suggesting that a mix of fat and carbohydrates were utilised as fuel. By contrast, the RER of Ser251 mice was close to 0.9, indicating that more carbohydrates were utilised as fuel (Fig. 6D).

PLIN2-Pro251 was not associated with NAFLD and metabolic diseases in humans

Data for 11,174 participants were available in the PMBB. The minor allele frequency of *PLIN2-Pro251* was approximately 5% in White participants and approximately 2% in Black participants.

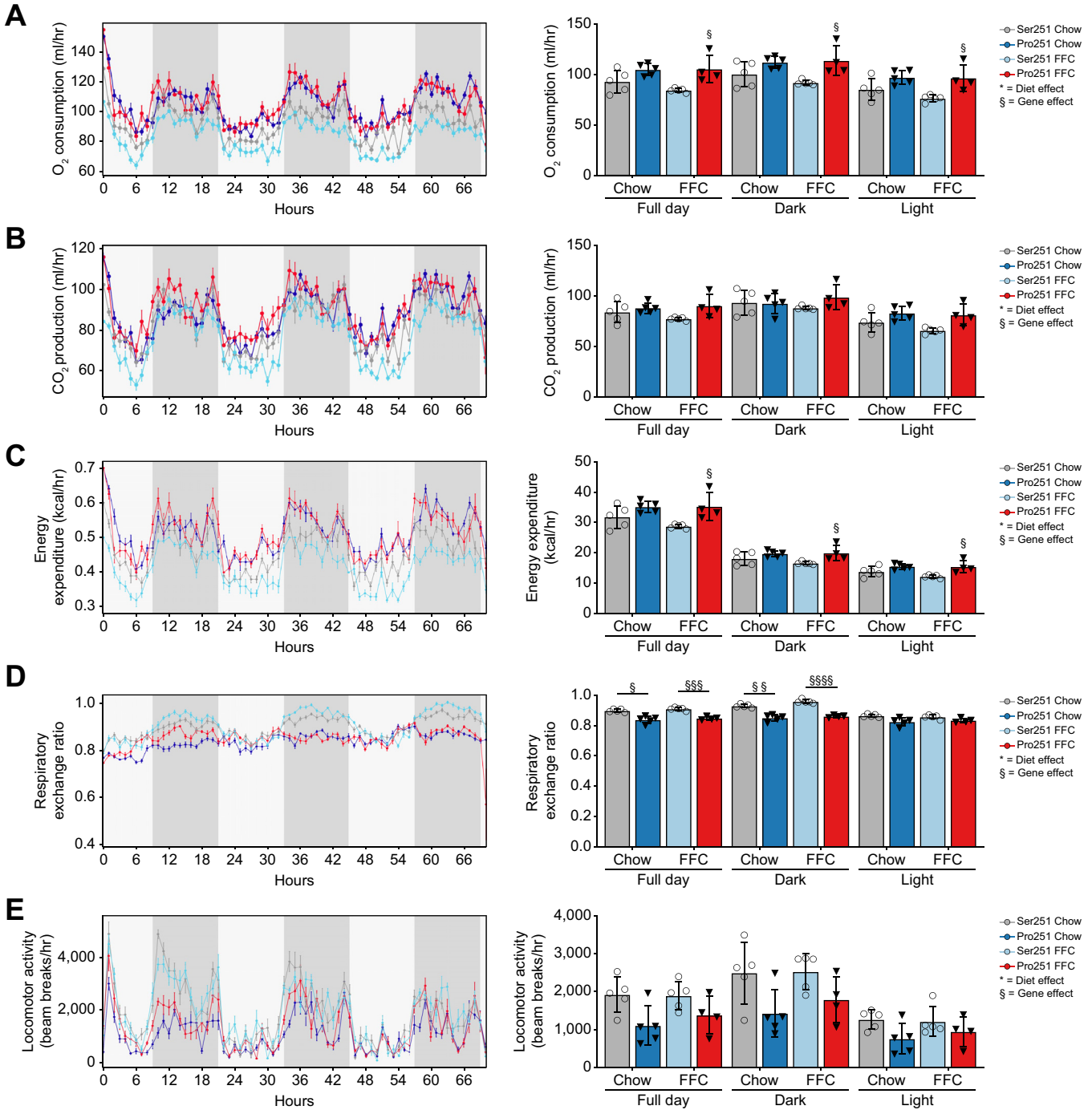

Fig. 6. Impact of *Pro251* on metabolic phenotype. *Pro251* had positive effect on metabolic phenotyping in both diets (A–C and E). *Pro251* had a decrease in respiratory exchange ratio in full day and dark (D). Statistical analyses were performed using a two-tailed unpaired *t*-test or one-way ANOVA with Tukey's *post-hoc* test. *Statistical difference between diets, *p <0.05; **p <0.005; ***p <0.0005; ****p <0.0001. §Statistical difference between genotypes, §p <0.05; §§p <0.005; §§§p <0.0005; §§§§p <0.0001. FFC, high-fat, high-fructose, high-cholesterol.

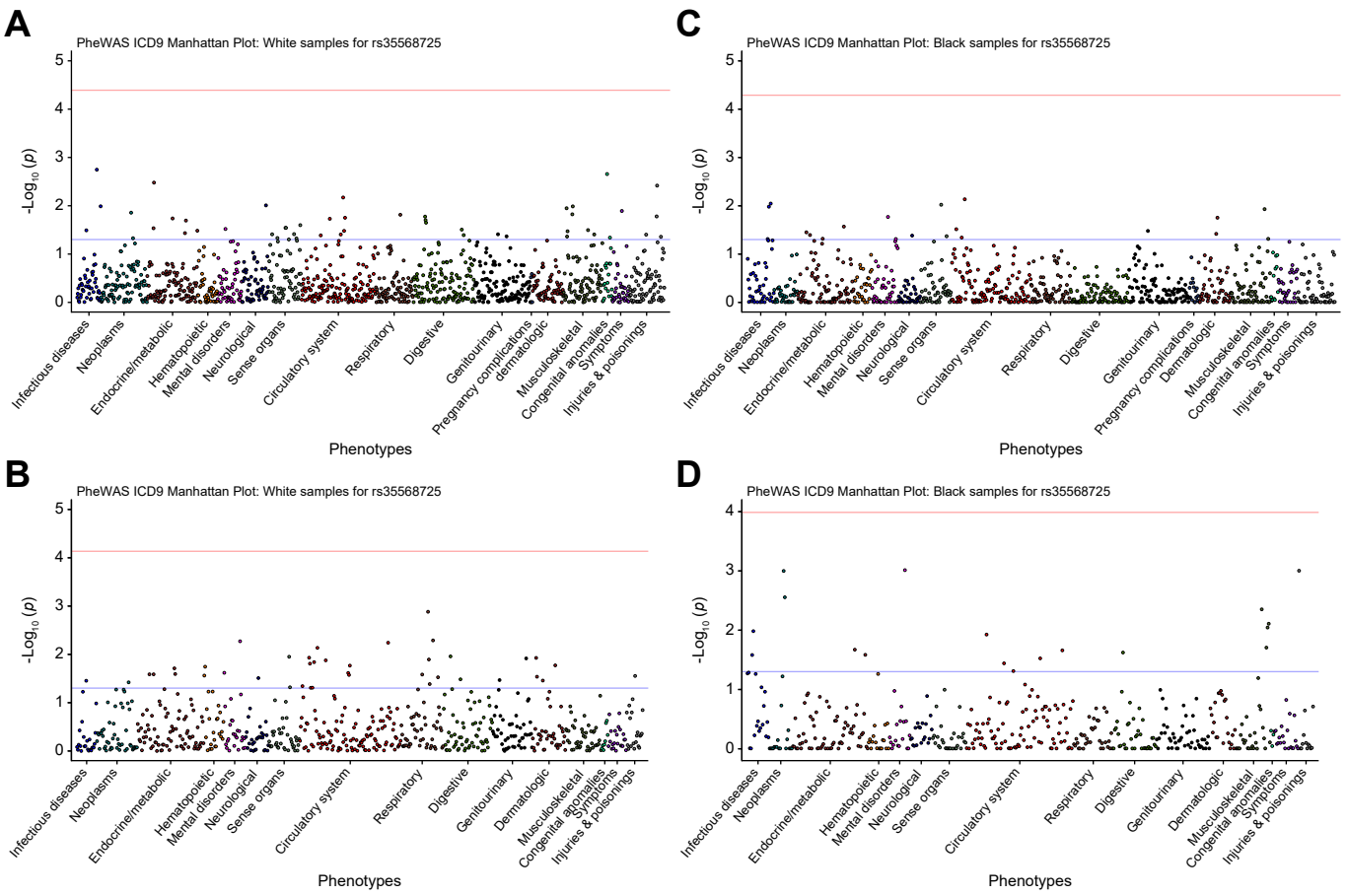

Fig. 7. Multivariable PheWAS of the effect of Pro251 on clinical phenotypes. Multivariable PheWAS of the effect of Pro251 on clinical phenotypes for White population (A and B). Multivariable PheWAS of the effect of Pro251 on clinical phenotypes for African American population (C and D). The line marks the Bonferroni significant cut-off. PheWAS, phenome-wide association study.

We identified a total of 296 ICD-10 code diagnoses of NAFLD and 10,878 controls. The PheWAS showed no association between homozygous *PLIN2-Pro251* and diagnosis of NAFLD or other severe liver diseases (Fig. 7A–D).

Similarly, in the MVP, the minor allele frequency of *PLIN2-Pro251* was approximately 5% in White participants and approximately 2% in Black, Hispanic, and Asian participants (n = 13,690) (Table S2). We further analysed the MVP dataset to identify whether there were associations between homozygous *PLIN2-Pro251*, NAFLD, and metabolic diseases. We did not find any association between *PLIN2-Pro251* carriers and increased risk of NAFLD or other severe liver diseases (Table 1). In addition, we found that homozygous *PLIN2-Pro251* had a trend towards a higher risk of cardiomyopathy and type 2 diabetes compared with non-carriers. However, these associations were not significant when adjusted with the Bonferroni correction (Table S3).

Table 1. Impact of the variant on phenotypes related to more severe liver disease.

Phenotype	Beta	SE	*p* value
HCC	1.933e-01	1.383e-01	0.16226
Cirrhosis	2.389e-01	1.562e-01	0.12624

Multivariable analyses adjusted for age, sex, BMI, and PC1-10.
HCC, hepatocellular carcinoma.

In the UKB, the minor allele frequency of *PLIN2-Pro251* was again approximately 5%. We further examined this dataset to determine the phenotypic and metabolic profile of *PLIN2-Pro251* carriers (n = 21,951.9) compared with non-carriers (n = 439,038). We analysed data from 30,359 UKB participants who had MRI-derived imaging (adjusted for age and BMI). Notably, we found that homozygous *PLIN2-Pro251* carriers had a trend towards reduced liver fat percentage (β = -0.15; SE = 0.08; p = 0.05) (Table 2); these data are especially notable as they are consistent with the results of our mouse model. Our analysis (adjusted for age and BMI) of the UKB also showed that homozygous *PLIN2-Pro251* carriers were associated with a significant reduction in visceral adipose tissue (β = -0.04; SE = 0.02; p = 0.04) and a trend towards increase in liver iron (β = 1.7; SE = 0.8; p = 0.05) (Table 2). We repeated the analysis to investigate the liver phenotype of the *PLIN2-Pro251* by adjusting for age and BMI in males and females. We found that the *PLIN2-Pro251* was associated with a trend towards a decrease in MRI-PDFF in males (β = -0.2; SE = 0.1; p = 0.06) but not in females (Table 2). In addition, there was a significant association between *PLIN2-Pro251* and decrease in visceral adipose tissue in all individuals. However, this association was not significant when considering males and females separately (Table S4). Moreover, these patients had increased levels of large and very large VLDL particles compared with non-carriers. The sex stratification of the lipidomic profile suggested a

Table 2. Association between *PLIN2-Pro251* and MRI-PDFF liver phenotype in the UKB adjusted for age and BMI.

Phenotype	Beta	SE	*p* value
All participants (N = 30,359)			
Liver volume	-5.251e-03	3.848e-03	0.17245
Subcutaneous fat volume	-0.0539815	0.0374349	0.149308
Visceral adipose tissue	**-0.0481373**	**0.0238025**	**0.0431**
MRI-PDFF	**-0.1570789**	**0.0819436**	**0.055258**
Liver iron	**1.726799**	**0.876434**	**0.048818**
HCC	1.933e-01	1.383e-01	0.16226
Cirrhosis	2.389e-01	1.562e-01	0.12624
Females (n = 14,645)			
Liver volume	-7.612e-03	4.861e-03	0.117
Subcutaneous fat volume	-0.0614021	0.0559731	0.272
Visceral adipose tissue	-0.0349735	0.0246701	0.156
MRI-PDFF	-0.0591458	0.1072458	0.581
Liver iron	1.633119	1.191840	0.170
HCC	3.262e-01	2.322e-01	0.160
Cirrhosis	3.105e-01	2.593e-01	0.231
Males (n = 15,714)			
Liver volume	-1.922e-04	5.979e-03	0.974
Subcutaneous fat volume	-0.0705943	0.0484526	0.145
Visceral adipose tissue	-3.518e-02	3.945e-02	0.372
MRI-PDFF	**-0.226995**	**0.124209**	**0.067**
Liver iron	1.948e+00	1.288e+00	0.130
HCC	1.500e-01	1.636e-01	0.359
Cirrhosis	0.168310	0.211089	0.425

Multivariable analyses adjusted for age, sex, BMI, and PC1-10. Values in bold denote statistical significance.
HCC, hepatocellular carcinoma; PDFF, proton density fat fraction.

difference in the male group compared with female, confirming an increase in lipid secretion, and suggesting a reduction in lipid accumulation in the liver (Fig. S5A–C).

We also tested the additive model in the MVP and in the UKB and we did not find any significant association between *PNPL2-Pro251* allele and risk of liver disease and lipidomic profile (data not shown).

Discussion

Our study shows that after 12 weeks of an FFC diet, hepatocyte-specific expression of human PLIN2-Pro251 in mice lacking *Plin2* is protective against macrosteatosis and liver TG accumulation. These improvements in metabolism were in part derived from higher energy expenditure, as evidenced by calorimetry data showing that Pro251 mice had an increase in O_2 consumption and RER. We found that Pro251 mice exhibited a trend towards increased acylcarnitine levels and a 4.4-fold increase in Acsbg1 (Acyl-CoA Synthetase, Bubblegum Family, member 1) gene expression (adjusted p = 0.045). Acylcarnitines are produced through the conjugation of acyl-CoAs with carnitine, which facilitates the transport of long-chain fatty acids across the inner mitochondrial membrane for β-oxidation. Recently, it has been demonstrated that acylcarnitine is involved in energy mobilisation and stimulates energy expenditure. Acsbg1-dependent fatty acyl-CoA synthesis plays a crucial role in controlling mitochondrial respiratory capacity and participates in the oxidation of long-chain saturated and unsaturated fatty acids. Consequently, the increased expression of Acsbg1 and the trend towards elevated acylcarnitine levels might have an impact on increasing energy expenditure.[23,24] Additional results from our lipidomic data also revealed that Pro251 mice have 47% less liver TG accumulation and a trend towards a decrease in liver DG compared with Ser251 mice. Moreover, the liver lipidomic composition of Pro251 mice showed a reduction in PUFA-TGs compared with Ser251 mice, indicating that there was less accumulation of PUFAs in the hepatic LD lipid core of Pro251 mice compared with Ser251 mice. Congruent with these data were our RNA-seq data which demonstrated reduced expression of genes involved in the epoxygenase pathway, thus supporting the hypothesis that there is less oxidative stress and less PUFA peroxidation in Pro251 mice compared with Ser251 mice. It is also possible that Pro251 mice produce fewer oxidised eicosanoids compared with Ser251 mice, thereby leading to an accumulation of PUFA species in the cytosol.[25] The reduction in PUFA-TGs that we observed in Pro251 mice is consistent with recent evidence showing that PUFAs redistribute into the LD core during oxidative stress.[25,26]

In accordance with previous literature, we noticed an increase in gene expression associated with *de novo* lipogenesis, in both Ser251 and Pro251 mice on the FFC diet.[27] However, mice expressing the *PLIN2-Pro*251 had less increase in lipogenic genes compared with Ser251 mice. In particular, Pro251 mice on the FFC diet had reduced mRNA expression of *Dgat2* and *Fasn* which are genes that have significant roles in *de novo* lipogenesis.[28] However, we did not observe a significant reduction in DGAT2 protein expression.

The mechanisms linking *PLIN2-Pro251* to the downregulation of mRNA expression of *Dgat2* and *Fasn* are not clear. The downregulation of *Dgat2* gene expression might reduce the gene expression of *Fasn*, resulting in a reduction of *de novo* lipogenesis and ultimately in less accumulation of liver TGs. This hypothesis is consistent with previous literature. A recent paper has shown that liver specific *Dgat2*-KO (knockout) mice have reduced expression of genes associated with *de novo* lipogenesis and especially a downregulation of *Fasn*. This was associated with a reduction in liver TG accumulation.[27] There is also evidence illustrating that *DGAT1*/*DGAT2* double KO cells treated with oleic acid accumulate less TG and fewer LDs than wild-type control cells.[29] This same study also demonstrated that *DGAT1/DGAT2* double KO cells, when treated with oleic acid, showed reduced accumulation of PLIN2 protein. Interestingly, this occurred despite these cells maintaining PLIN2 mRNA levels similar to those found in wild-type cells. This suggests a potential genetic interaction between *DGAT2* and *PLIN2*.[29] PLIN2 protein has two structural domains: (1) the N-terminal domain that contains amphipathic alpha-helices that modulate the binding of the protein to lipid droplets; and (2) the C-terminal four-helix bundle domain that interacts with membranes and other proteins. With regard to the latter, the substitution of a serine-to-proline residue in position aa 251 observed in PLIN2-Pro251 might disrupt the hydrogen bonding of the PLIN2 protein peptide backbone and induce a kink in the helix, altering the organisation of the four-helix bundle (Fig. S6). This alteration to the C-terminal four-helix bundle domain might affect the phosphorylation capacity of PLIN2-Pro251 and inhibit its interaction with other proteins. Further studies are warranted to gain a better understanding of the role of PLIN2 and its interaction with other proteins.

Our analysis of three independent biobank datasets of diverse, international populations encompasses the largest study to date of *PLIN2-Pro251*. We found that this variant is rare with an overall prevalence of 2% in Black, Hispanic, and Asian populations and 5% in White populations. Our PheWAS analyses revealed that individuals homozygous for this gene variant

exhibit a mixed metabolic risk profile but no association with a clinical diagnosis of NAFLD or more severe liver diseases. Interestingly, we observed trends toward lower liver fat as diagnosed by magnetic resonance spectroscopy and lower subcutaneous and visceral adiposity in all individuals and in males, but not in females. This suggests that the influence of the *PLIN2-Pro251* variant on hepatic steatosis may be secondary to its effect on visceral fat accumulation, rather than a direct effect on hepatic lipid metabolism. It is noteworthy that the present experimental mouse model, which specifically expressed *PLIN2-Pro251* in the liver in a full *Plin2* KO context, could not address this question. Conversely, we detected trends toward higher risk of cardiometabolic disorders such as cardiomyopathy, ischaemic heart disease, and type 2 diabetes, as well as increased risk of large and very-large circulating VLDL particles. These results are consistent with those of our mouse model, where we saw a trend towards an increase in VLDL liver secretion in Pro251 mice compared with Ser251 mice.

The findings of our human data analyses appear to be in contrast with two previous clinical studies finding that *PLIN2-Pro251* was significantly associated with NASH, with an allelic odds ratio of 2.98[17] and that a cohort of Italian women with *PLIN2-Pro251* and obesity-associated metabolic alterations had significantly lower insulin levels, respectively.[30] Nevertheless, we note that both these studies involved small cohorts and that the association between *PLIN2-Pro251* and NASH was based on only three homozygous carriers of this genetic variant.

In conclusion, our study suggests that *PLIN2-Pro251* protects against hepatic steatosis through the downregulation of lipid synthetic and epoxygenase genes, and the alteration of LD and liver lipids. Counterintuitively, this genetic variant also appears to increase cardiometabolic risk perhaps through the promotion of VLDL production. As there is presently very limited knowledge and understanding of how liver lipid species confer cardiometabolic risk, further research is warranted including an extension of the feeding duration to investigate the trajectory and durability of our findings on lipid and glucose metabolism. More broadly, our study confirms that a comprehensive understanding of the biology of LDs in hepatocytes and other liver cells is necessary to comprehend the molecular mechanisms and heterogeneity of NAFLD and other steatotic diseases.

Abbreviations

Acsbg1, Acyl-CoA Synthetase, Bubblegum Family, member 1; ALT, alanine aminotransferase; DEGs, differentially expressed genes; DG, diacylglycerol; EHR, electronic health record; EtOH, ethanol; FFC diet, high-fat; high-fructose, high-cholesterol diet; GTT, glucose tolerance test; HCC, hepatocellular carcinoma; ITT, insulin tolerance test; KO, knockout; LD, lipid droplet; MVP, Million Veteran Program; NAFLD, non-alcoholic fatty liver disease; NASH, non-alcoholic steatohepatitis; NEFA, non-esterified fatty acid; PDFF, proton density fat fraction; PheWAS, phenome-wide association study; PLIN2, Perilipin 2; PMBB, Penn Medicine BioBank; PUFA-TG, polyunsaturated-fatty-acids-TG; qPCR, quantitative real-time PCR; RER, respiratory exchange ratio; TGs, triglycerides; UKB, UK Biobank.

Financial support

This work was supported by the USA AASLD Afdhal/McHutchison LIFER Award (ES); USA NIH T32-DK007742 (JD); USA NIH 1R01AA026302 (RC). CVS is supported by the NRW Rueckkehr Programme of the Ministry of Culture and Science of the German State of North Rhine-Westphalia, Germany (Europe). MG is supported by the Burroughs Wellcome Fund (USA).

Conflicts of interest

The authors declare no conflicts of interest that pertain to this work.

Please refer to the accompanying ICMJE disclosure forms for further details.

Authors' contributions

Conceptualisation: ES, RC. Methodology: ES, RC. Formal analysis: ES. Investigation: ES. Data collection: ES. Data curation: YS, SJ, DGB, CL, EEF, JLD, DC, CAM. Software: CVS, BEH, MV. Validation: ES, CVS, BEH, MV. Formal analysis: CVS, BEH, MV. Visualisation: YS, SJ, DGB, CL, EEF, JLD, DC, CAM, KTC, JTB, NJH, DEK, KMC, PST, JAL, JH, SB, MG, MCP. Writing – original draft: ES. Writing – review and editing: all authors. Project administration: ES. Resources: DJR, RC. Supervision: DJR, RC. Funding acquisition: ES, RC.

Data availability statement

Research data that documents, supports and validates the research findings will be made available after the main findings from the final research data set have been accepted for publication.

Acknowledgements

The authors would like to thank Dr Kenton Woodard for the generation of the liver-specific vector (Penn Vector Core and Gene Therapy Program, University of Pennsylvania); Dr Jonathan Schug and Dr John Tobias for expert technical support. Special thanks also to the Center for Molecular Studies in Digestive and Liver Diseases (NIH P30 DK050306) and its core facilities (Molecular Pathology and Imaging Core, Molecular Biology).

This research has been conducted using the UK Biobank Resource under Application Number 70653. UK biobank data was accessed by C.V.S and D.J.R.. Copyright © 2023, NHS England. Re-used with the permission of the NHS England and/or UK Biobank. All rights reserved. This work uses data provided by patients and collected by the NHS as part of their care and support.

Supplementary data

Supplementary data to this article can be found online at https://doi.org/10.1016/j.jhepr.2023.100902.

References

[1] Scorletti E, Carr RM. A new perspective on NAFLD: focusing on lipid droplets. J Hepatol 2022;76:934–945.
[2] Paik JM, Henry L, De Avila L, Younossi E, Racila A, Younossi ZM. Mortality related to nonalcoholic fatty liver disease is increasing in the United States. Hepatol Commun 2019;3:1459–1471.
[3] Diehl AM, Day C. Cause, pathogenesis, and treatment of nonalcoholic steatohepatitis. N Engl J Med 2017;377:2063–2072.
[4] Sherif ZA, Saeed A, Ghavimi S, Nourie S-M, Laiyemo AO, Brim H, et al. Global epidemiology of nonalcoholic fatty liver disease and perspectives on US minority populations. Dig Dis Sci 2016;61:1214–1225.
[5] Thiam AR, Farese Jr RV, Walther TC. The biophysics and cell biology of lipid droplets. Nat Rev Mol Cell Biol 2013;14:775–786.
[6] Carr RM, Ahima RS. Pathophysiology of lipid droplet proteins in liver diseases. Exp Cell Res 2016;340:187–192.
[7] Najt CP, Senthivinayagam S, Aljazi MB, Fader KA, Olenic SD, Brock JRL, et al. Liver-specific loss of Perilipin 2 alleviates diet-induced hepatic steatosis, inflammation, and fibrosis. Am J Physiol Gastrointest Liver Physiol 2016;310:G726–G738.
[8] Carr RM, Dhir R, Mahadev K, Comerford M, Chalasani NP, Ahima RS. Perilipin staining distinguishes between steatosis and nonalcoholic steatohepatitis in adults and children. Clin Gastroenterol Hepatol 2017;15:145–147.
[9] Carr RM, Peralta G, Yin X, Ahima RS. Absence of perilipin 2 prevents hepatic steatosis, glucose intolerance and ceramide accumulation in alcohol-fed mice. PLoS One 2014;9:e97118.
[10] Libby AE, Bales E, Orlicky DJ, McManaman JL. Perilipin-2 deletion impairs hepatic lipid accumulation by interfering with sterol regulatory element-

binding protein (SREBP) activation and altering the hepatic lipidome. J Biol Chem 2016;291:24231–24246.
[11] McManaman JL, Bales ES, Orlicky DJ, Jackman M, MacLean PS, Cain S, et al. Perilipin-2-null mice are protected against diet-induced obesity, adipose inflammation, and fatty liver disease. J Lipid Res 2013;54:1346–1359.
[12] Williams B, Correnti J, Oranu A, Lin A, Scott V, Annoh M, et al. A novel role for ceramide synthase 6 in mouse and human alcoholic steatosis. FASEB J 2018;32:130–142.
[13] Imai Y, Boyle S, Varela GM, Caron E, Yin X, Dhir R, et al. Effects of perilipin 2 antisense oligonucleotide treatment on hepatic lipid metabolism and gene expression. Physiol Genomics 2012;44:1125–1131.
[14] Mann JP, Romeo S, Valenti L. Lipid droplets as the genetic nexus of fatty liver. Liver Int 2022;42:2594–2596.
[15] Bianco C, Jamialahmadi O, Pelusi S, Baselli G, Dongiovanni P, Zanoni I, et al. Non-invasive stratification of hepatocellular carcinoma risk in non-alcoholic fatty liver using polygenic risk scores. J Hepatol 2021;74:775–782.
[16] Magne J, Aminoff A, Perman Sundelin J, Mannila MN, Gustafsson P, Hultenby K, et al. The minor allele of the missense polymorphism Ser251Pro in perilipin 2 (PLIN2) disrupts an alpha-helix, affects lipolysis, and is associated with reduced plasma triglyceride concentration in humans. FASEB J 2013;27:3090–3099.
[17] Faulkner CS, White CM, Shah VH, Jophlin LL. A single nucleotide polymorphism of PLIN2 is associated with nonalcoholic steatohepatitis and causes phenotypic changes in hepatocyte lipid droplets: a pilot study. Biochim Biophys Acta Mol Cell Biol Lipids 2020;1865:158637.
[18] Ganz M, Bukong TN, Csak T, Saha B, Park J-K, Ambade A, et al. Progression of non-alcoholic steatosis to steatohepatitis and fibrosis parallels cumulative accumulation of danger signals that promote inflammation and liver tumors in a high fat-cholesterol-sugar diet model in mice. J Transl Med 2015;13:193.
[19] Gaziano JM, Concato J, Brophy M, Fiore L, Pyarajan S, Breeling J, et al. Million Veteran Program: a mega-biobank to study genetic influences on health and disease. J Clin Epidemiol 2016;70:214–223.
[20] Klarin D, Damrauer SM, Cho K, Sun YV, Teslovich TM, Honerlaw J, et al. Genetics of blood lipids among ~300,000 multi-ethnic participants of the Million Veteran Program. Nat Genet 2018;50:1514–1523.
[21] Correnti J, Lin C, Brettschneider J, Kuriakose A, Jeon S, Scorletti E, et al. Liver-specific ceramide reduction alleviates steatosis and insulin resistance in alcohol-fed mice. J Lipid Res 2020;61:983–994.
[22] Tippetts TS, Holland WL, Summers SA. The ceramide ratio: a predictor of cardiometabolic risk. J Lipid Res 2018;59:1549–1550.
[23] Simcox J, Geoghegan G, Maschek JA, Bensard CL, Pasquali M, Miao R, et al. Global analysis of plasma lipids identifies liver-derived acylcarnitines as a fuel source for brown fat thermogenesis. Cell Metab 2017;26:509–522.e6.
[24] Kanno T, Nakajima T, Kawashima Y, Yokoyama S, Asou HK, Sasamoto S, et al. Acsbg1-dependent mitochondrial fitness is a metabolic checkpoint for tissue T(reg) cell homeostasis. Cell Rep 2021;37:109921.
[25] Bailey AP, Koster G, Guillermier C, Hirst EMA, MacRae JI, Lechene CP, et al. Antioxidant role for lipid droplets in a stem cell niche of *Drosophila*. Cell 2015;163:340–353.
[26] Rogers S, Gui L, Kovalenko A, Zoni V, Carpentier M, Ramji K, et al. Triglyceride lipolysis triggers liquid crystalline phases in lipid droplets and alters the LD proteome. J Cell Biol 2022;221:e202205053.
[27] Gluchowski NL, Gabriel KR, Chitraju C, Bronson RT, Mejhert N, Boland S, et al. Hepatocyte deletion of triglyceride-synthesis enzyme acyl CoA: diacylglycerol acyltransferase 2 reduces steatosis without increasing inflammation or fibrosis in mice. Hepatology 2019;70:1972–1985.
[28] Strable MS, Ntambi JM. Genetic control of de novo lipogenesis: role in diet-induced obesity. Crit Rev Biochem Mol Biol 2010;45:199–214.
[29] Xu S, Zou F, Diao Z, Zhang S, Deng Y, Zhu X, et al. Perilipin 2 and lipid droplets provide reciprocal stabilization. Biophys Rep 2019;5:145–160.
[30] Sentinelli F, Capoccia D, Incani M, Bertoccini L, Severino A, Pani MG, et al. The perilipin 2 (PLIN2) gene Ser251Pro missense mutation is associated with reduced insulin secretion and increased insulin sensitivity in Italian obese subjects. Diabetes Metab Res Rev 2016;32:550–556.

Journal of Hepatology, Volume *6*

Supplemental information

A missense variant in human perilipin 2 (*PLIN2* Ser251Pro) reduces hepatic steatosis in mice

Eleonora Scorletti, Yedidya Saiman, Sookyoung Jeon, Carolin V. Schneider, Delfin G. Buyco, Chelsea Lin, Blanca E. Himes, Clementina A. Mesaros, Marijana Vujkovic, Kate Townsend Creasy, Emma E. Furth, Jeffrey T. Billheimer, Nicholas J. Hand, David E. Kaplan, Kyong-Mi Chang, Philip S. Tsao, Julie A. Lynch, Joseph L. Dempsey, Julia Harkin, Susovon Bayen, Donna Conlon, Marie Guerraty, Michael C. Phillips, Daniel J. Rader, and Rotonya M. Carr

A missense variant in human perilipin 2 (*PLIN2* Ser251Pro) reduces hepatic steatosis in mice

Eleonora Scorletti, Yedidya Saiman, Sookyoung Jeon, Carolin V. Schneider, Delfin G. Buyco, Chelsea Lin, Blanca E. Himes, Clementina A. Mesaros, Marijana Vujkovic, Kate Townsend Creasy, Emma E. Furth, Jeffrey T. Billheimer, Nicholas J. Hand, David E. Kaplan, Kyong-Mi Chang, Philip S. Tsao, Julie A. Lynch, Joseph L. Dempsey, Julia Harkin, Susovon Bayen, Donna Conlon, Marie Guerraty, Michael C. Phillips, Daniel J. Rader, Rotonya M. Carr

Table of contents

Supplementary materials:

Animal experiment

Experiments were performed according to the protocols approved by the Institutional Animal Care and Use Committee of the University of Pennsylvania. All efforts were made to treat animals with humane care and minimize their discomfort. Mice were kept in barrier facilities (12-hour light/12-hour dark cycle) with *ad libitum* food and water, unless stated. Littermate controls were utilized.

*Adfp*D2–3 mice were provided by Dr. Palczewski. *Adfp*D2–3 mice lack exons 2 and 3 of the *Adfp* gene but do have mRNA expression of an unstable short-form *Adfp* (1). We crossed these mice from Balb/c to C57B6/J mice for more than ten generations. We called these mice *Plin2* KO-mice (1).

Sphingolipid and ceramide analyses

Liver tissue was homogenized in a RIPA buffer (50 mM Tris (pH 8.0), 150 mM NaCl, 5 mM EDTA, 1% v/v NP-40, 0.5% w/v sodium deoxycholate, 0.1% v/v SDS, 50 mM sodium fluoride). Protein concentrations were determined by BCA assay. Liver homogenate and plasma samples were analyzed by high performance liquid chromatography-tandem mass spectrometry for ceramide content at the Lipidomics Shared Resource at the Medical University of South Carolina. Hepatic ceramide data were normalized to total protein levels.

Lipidomic

Tissue preparation for lipids extraction

Sections of approximately 10 mg of frozen tissues were cut on a tile kept in dry ice with a new blade kept in dry ice. The tissue was added to a microcentrifuge tube with 0.6 mL 80% methanol (MeOH) and 20 µL on internal standard mix (1:1, SPLASH® LIPIDOMIX #330707 and Ceramide/Sphingoid Internal Standard Mixture I #LM6002, both from Avanti Polar Lipids, Alablaster, AL) and kept in dry ice. Samples were omogenised by pulse sonication (30 half-second pulse on ice) and incubated on ice for 20 min for metabolites extraction. Each tube was then vortexed 3x 30 seconds each. The tissue homogenates were then moved to a 10 mL glass borosilicate tube with a screw cap. The remaining tissue in the microcentrifuge tubes was rinsed into the glass tube with 0.5 mL MeOH. In each of the tubes, 5 mL methyl tert-butyl ether (MTBE) were added and then tubes were shaken vigorously for 30 min. In each tube, 1.2 mL water was added and then tubes vortexed for 30 sec each. Centrifugation for 10 min @ 1000xg created two phases. The top clear phase was moved to a clean glass Pyrex tube and dried down under

nitrogen. 100 µL MTBE/MeOH=1/3 (v/v) was used to re-suspend the residue. The sample was spun down at 10, 000 x g for 10 min at 4°C and only the top 50 µL were transferred to a HPLC vial for LC-MS analysis. A pooled sample was created by mixing 10 µL of each re-suspended sample. 2 µL injections were made.

Liquid chromatography high resolution -mass spectrometry (LC-HRMS) for lipids.

Metabolites were separated using a Ascentis Express C18, 2.1 × 150 mm 2.7µm column (Sigma-Aldrich, St. Louis, MO) on an UltiMate 3000 HPLC system. The metabolites were eluted on a 0.4 m/min flow-rate gradient using Solvent A (4:6 v/v water:acetonitrile, 0.1% formic acid, 10 mM ammonium formate) and Solvent B (1:9 v/v acetonitrile:isopropanol, 0.1% formic acid, 10 mM ammonium formate). The gradient was as follows: 10% B at 0 min, 10% B at 1 min, 40% B at 4 min, 75% B at 12 min, 99% B at 21 min, 99% B at 24 min, 10% B at 24.5 min, 10% at 30 min. Separations were performed at 55 °C.

For the HRMS analysis, a recently calibrated QE Exactive-HF mass spectrometer (Thermo Fisher Scientific) was used in positive ion mode with an HESI source. The operating conditions were: spray voltage at 3.5 kV; capillary temperature at 285°C; auxiliary temperature 370°C; tube lens 45. Nitrogen was used as the sheath gas at 45 units, the auxiliary gas at 10 units and sweep gas was 2 units. The same MS conditions were used in negative ionization mode, but with a spray voltage at 3.2 kV. Control extraction blanks were made in the same way using just the solvents instead of the tissue homogenate. The control blanks were used for the exclusion list with a threshold feature intensity set at 1e10^5. Untargeted analysis and targeted peak integration was conducted using LipidsSearch 4.2 (Thermo Fisher Scientific) as described by Wang et al (DOI: 10.4155/bio-2021-0098).

An external mass calibration was performed using the standard calibration mixture approximately every three days. All samples were analyzed in a randomized order in full scan MS that alternated with MS2 of top 20, with HCD scans at 30, 45 or 60 eV. Full scan resolution was set to 120,000 in the scan range between m/z 250–1800. The pool sample was run every 15 samples. Lipids quantification was done from the full scan data. The areas were normalized based on the amount of the internal standard added for each class (as found in the Table x1). All amounts were normalized to the original tissue weight.

Fig. S1

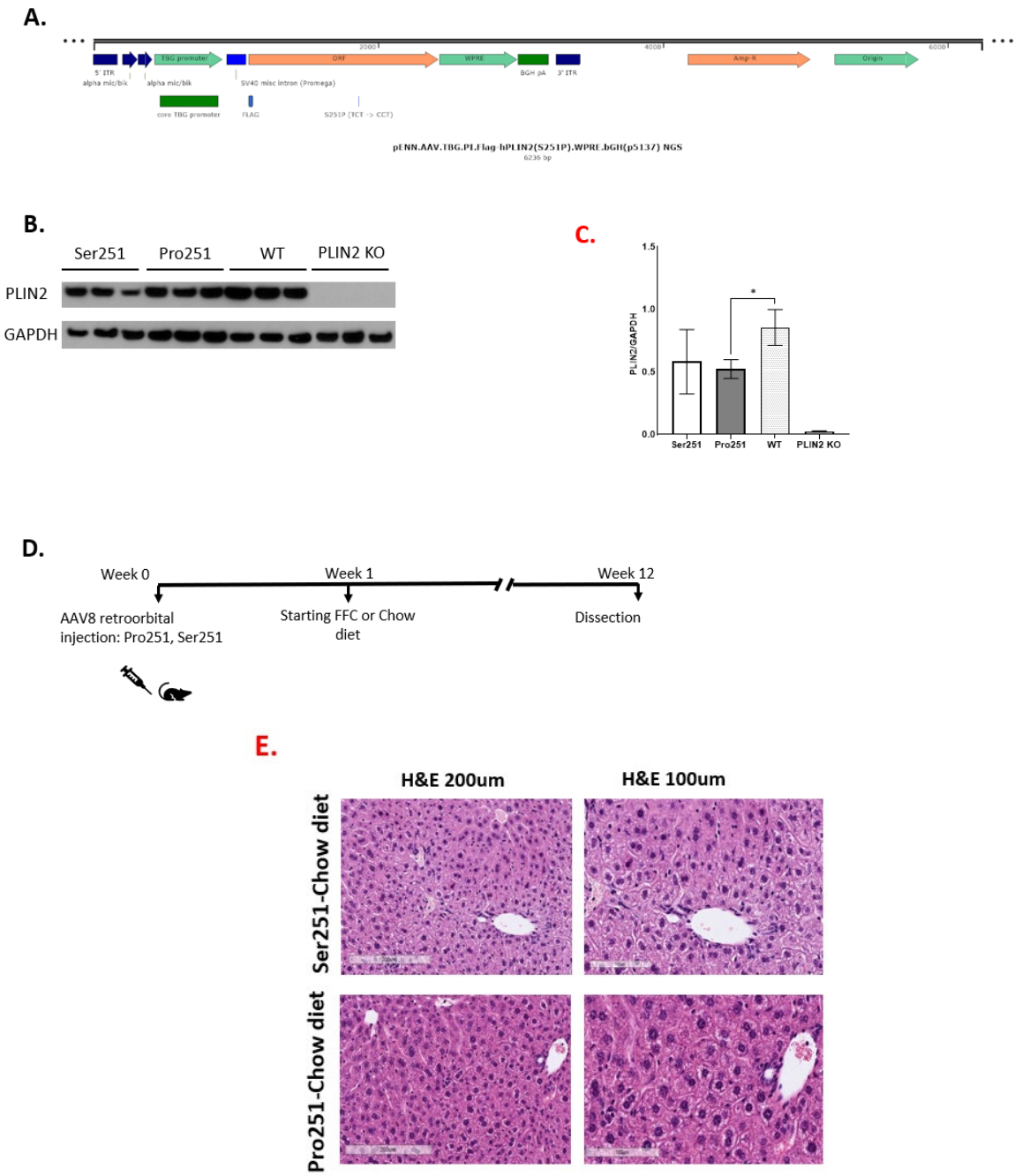

Generation of a mouse model of *Plin2*-Pro251 in hepatocytes and experimental design. Map of the *Plin2*-Pro251 plasmid (A), hepatic PLIN2 protein and mRNA expression (B-C), study design (D). Liver histology for the Pro251 and Ser251 groups on chow diet (E). PLIN2 relative protein

levels by Western Blotting were normalized to GAPDH (B and C). Statistical analyses were performed using a two-tailed unpaired *t*-test or one-way ANOVA with Tukey's posthoc test. *Indicates statistical difference between diets, *P < 0.05; **P < 0.005; ***P < 0.0005; ****P < 0.0001. §Indicates statistical difference between genotypes, §P < 0.05; §§P < 0.005; §§§P < 0.0005; §§§§P < 0.0001.

Fig. S2

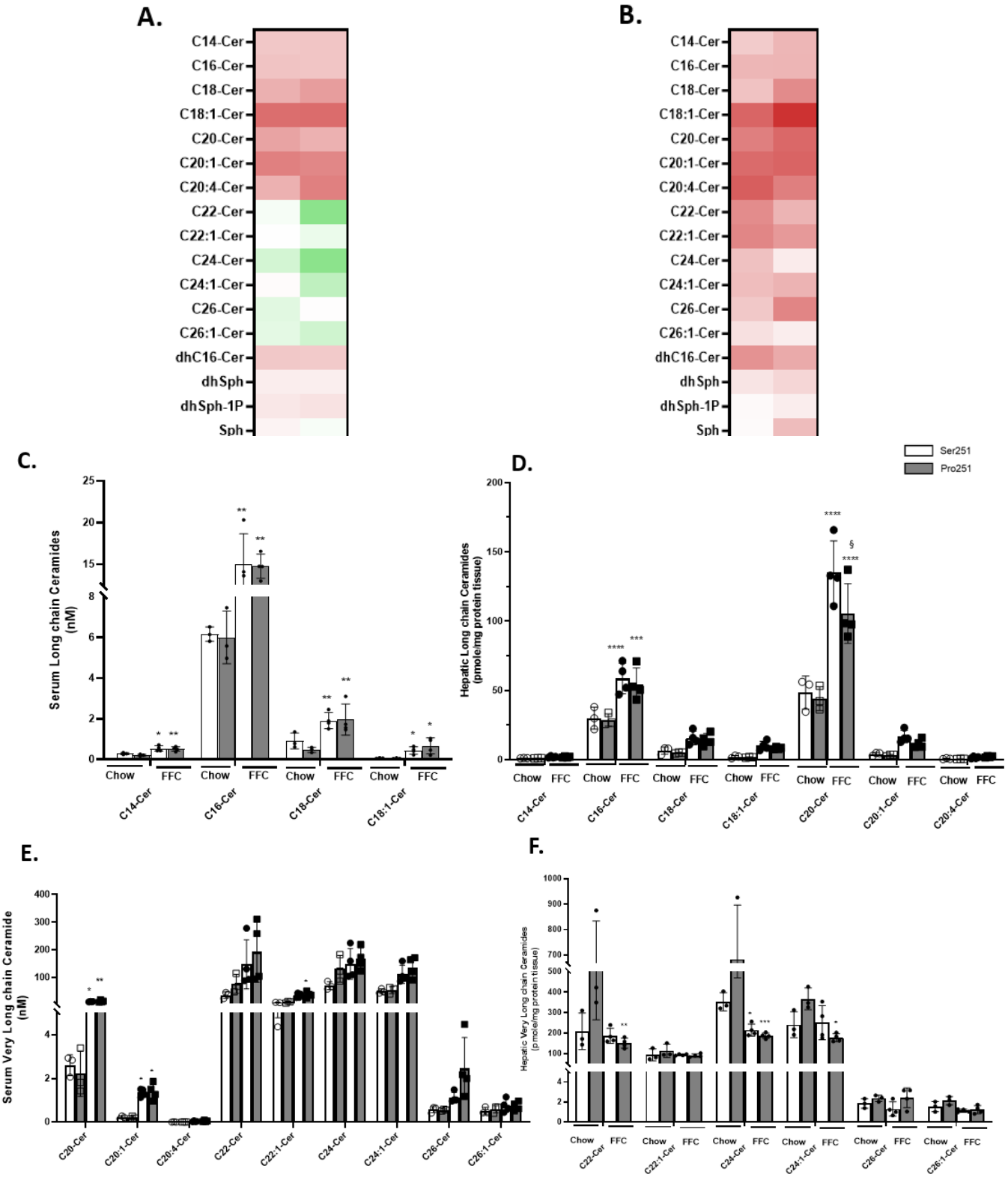
A.
B.
C14-Cer
C16-Cer
C18-Cer
C18:1-Cer
C20-Cer
C20:1-Cer
C20:4-Cer
C22-Cer
C22:1-Cer
C24-Cer
C24:1-Cer
C26-Cer
C26:1-Cer
dhC16-Cer
dhSph
dhSph-1P
Sph
C.
Serum Long chain Ceramides (nM)
D.
Hepatic Long chain Ceramides (pmole/mg protein tissue)
Ser251
Pro251
Chow
FFC
E.
Serum Very Long chain Ceramide (nM)
F.
Hepatic Very Long chain Ceramides (pmole/mg protein tissue)

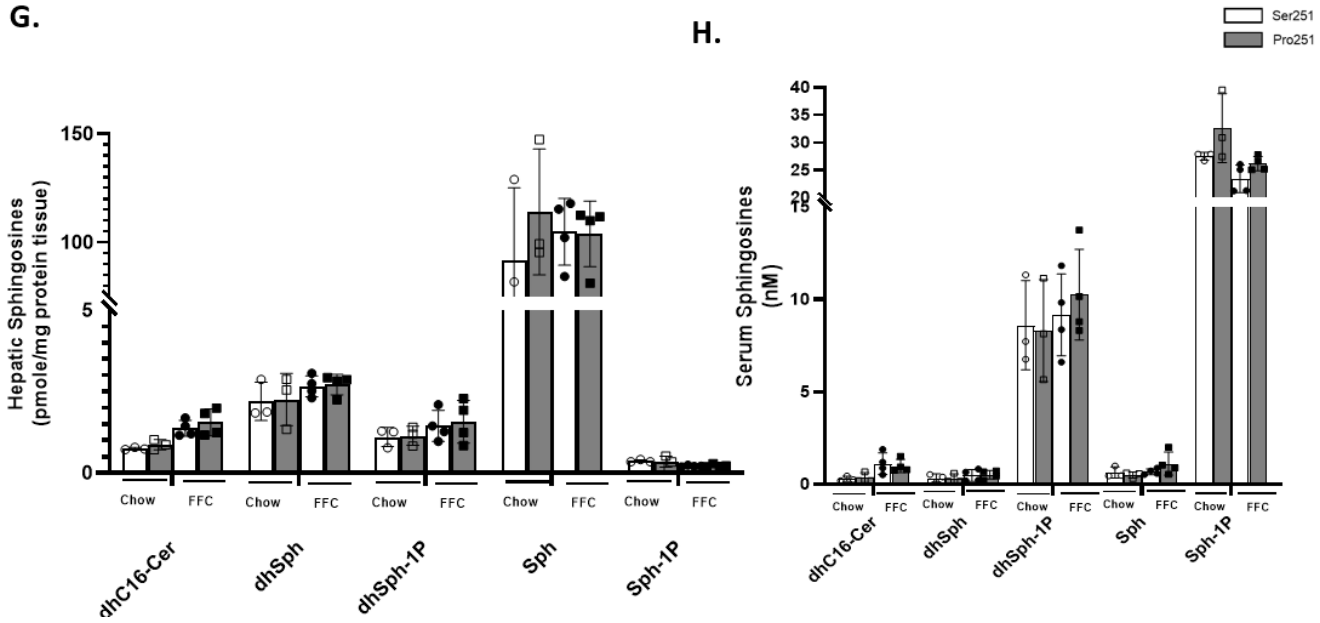

In the heatmap, the color code indicates the log2 of the ratio between means of the groups for an individual ceramide. A more intense red color indicates a greater increase of absolute concentration of the individual ceramide in the liver (A) and serum (B). Serum long chain ceramides (C), hepatic long chain ceramides (D), serum very long chain ceramides (E), hepatic very long chain ceramides (F), hepatic sphingolipids (G) and serum sphingolipids (H). Statistical analyses were performed using a two-tailed unpaired *t*-test or one-way ANOVA with Tukey's posthoc test. *Indicates statistical difference between diets, *P < 0.05; **P < 0.005; ***P < 0.0005; ****P < 0.0001. §Indicates statistical difference between genotypes, §P < 0.05; §§P < 0.005; §§§P < 0.0005; §§§§P < 0.0001.

Fig. S3

PLIN1, PLIN3 relative protein levels by Western Blotting were normalized to GAPDH (B and C).

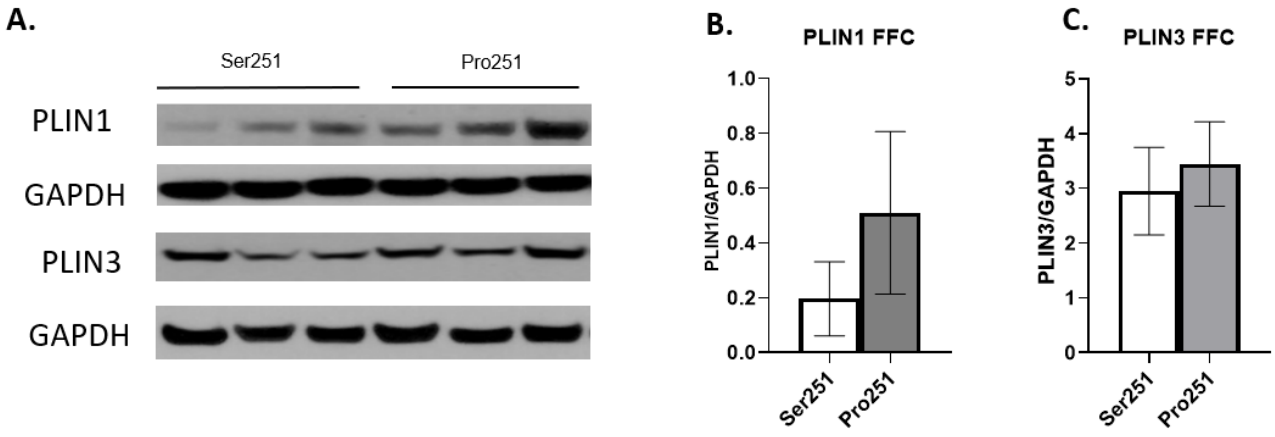

Statistical analyses were performed using a two-tailed unpaired *t*-test or one-way ANOVA with Tukey's posthoc test. *Indicates statistical difference between diets, *P < 0.05; **P < 0.005; ***P < 0.0005; ****P < 0.0001. §Indicates statistical difference between genotypes, §P < 0.05; §§P < 0.005; §§§P < 0.0005; §§§§P < 0.0001.

Fig. S4

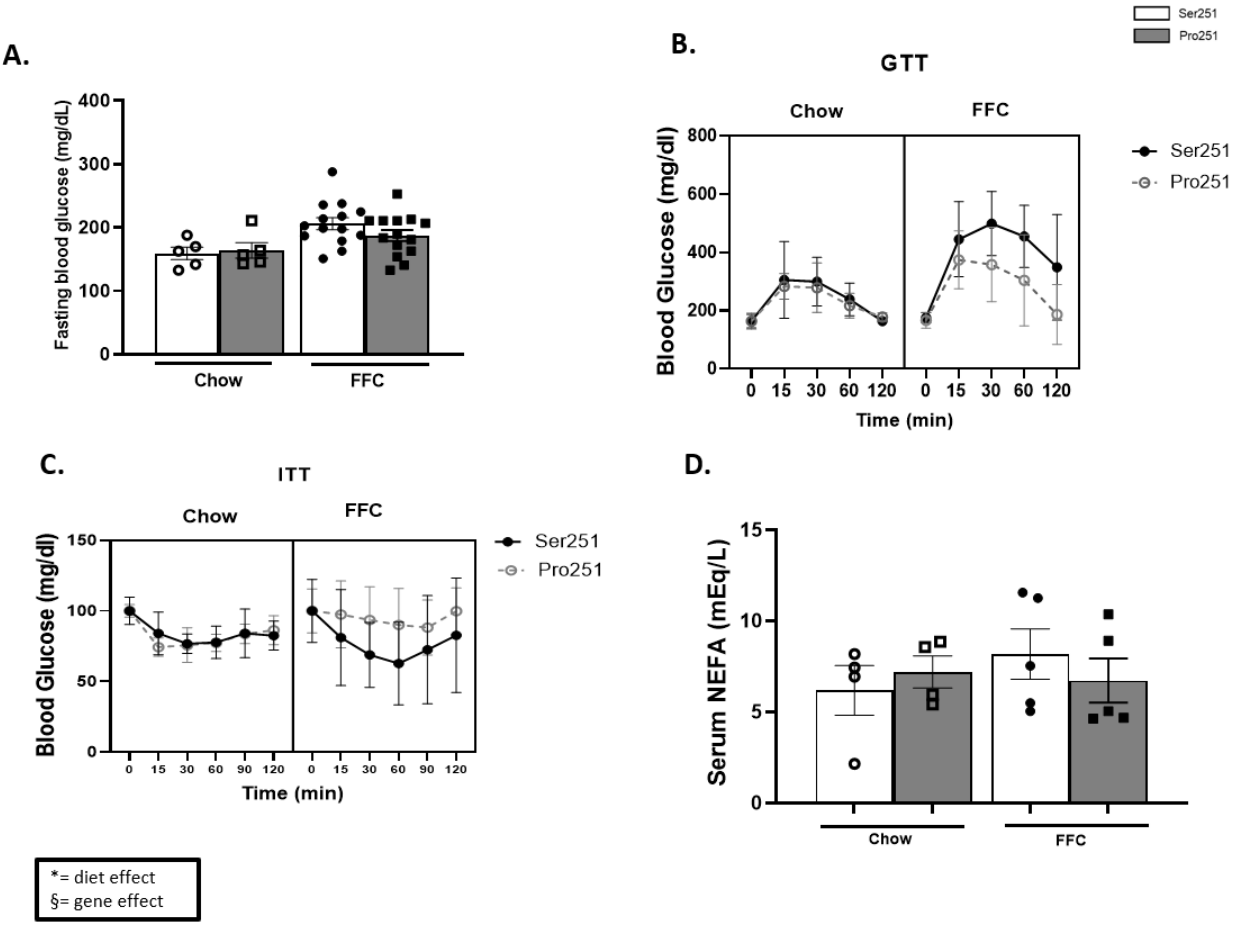

Fasting blood glucose (A), GTT (B), ITT (C), and serum NEFA (D). Statistical analyses were performed using a two-tailed unpaired *t*-test or one-way ANOVA with Tukey's posthoc test. *Indicates statistical difference between diets, *P < 0.05; **P < 0.005; ***P < 0.0005; ****P < 0.0001. §Indicates statistical difference between genotypes, §P < 0.05; §§P < 0.005; §§§P < 0.0005; §§§§P < 0.0001.

Fig. S5.

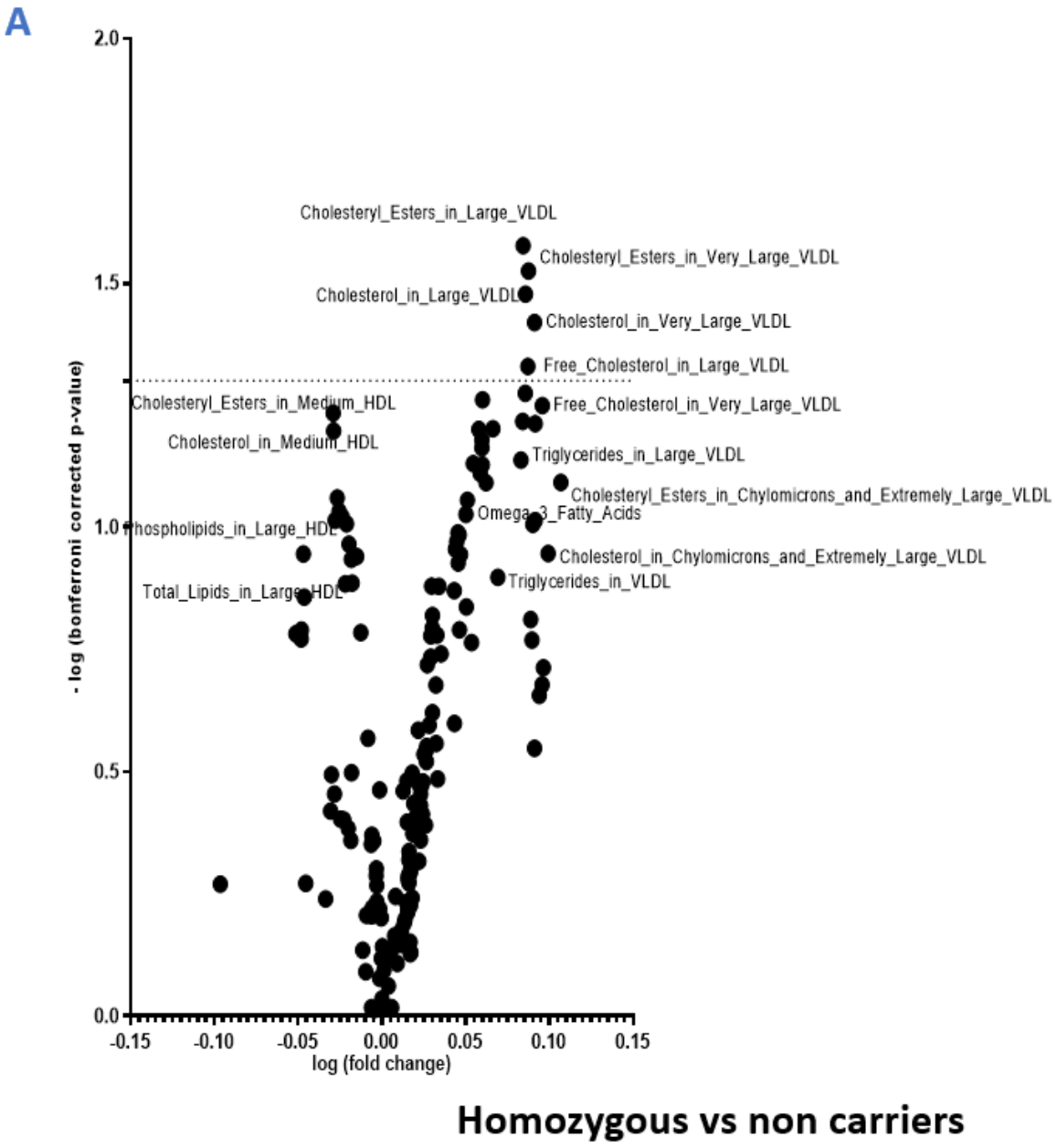
A
2.0
1.5
1.0
0.5
0.0
- log (bonferroni corrected p-value)
-0.15
-0.10
-0.05
0.00
0.05
0.10
0.15
log (fold change)
Cholesteryl_Esters_in_Large_VLDL
Cholesteryl_Esters_in_Very_Large_VLDL
Cholesterol_in_Large_VLDL
Cholesterol_in_Very_Large_VLDL
Free_Cholesterol_in_Large_VLDL
Cholesteryl_Esters_in_Medium_HDL
Free_Cholesterol_in_Very_Large_VLDL
Cholesterol_in_Medium_HDL
Triglycerides_in_Large_VLDL
Cholesteryl_Esters_in_Chylomicrons_and_Extremely_Large_VLDL
Omega_3_Fatty_Acids
Phospholipids_in_Large_HDL
Cholesterol_in_Chylomicrons_and_Extremely_Large_VLDL
Triglycerides_in_VLDL
Total_Lipids_in_Large_HDL
Homozygous vs non carriers

B.

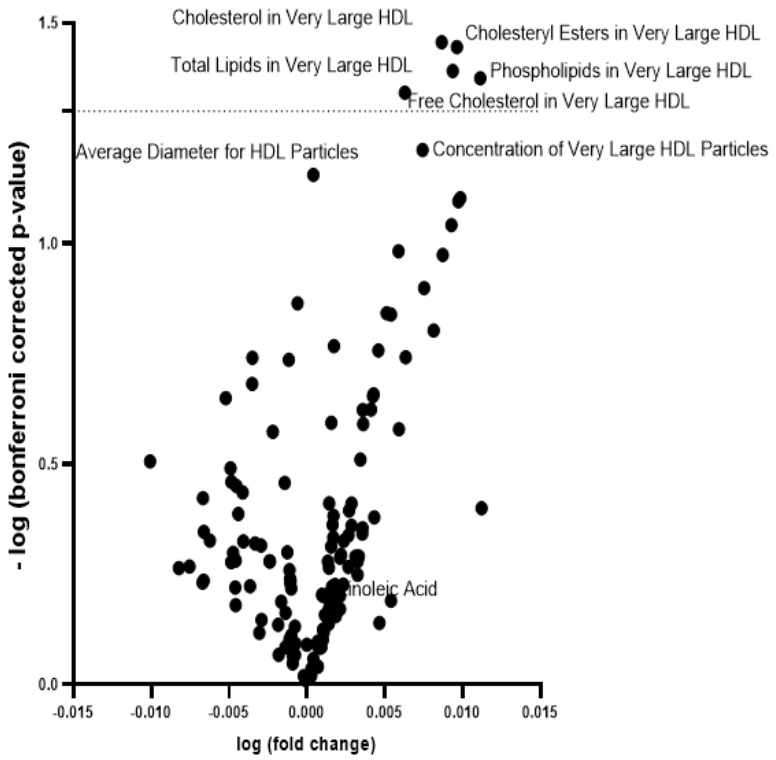

Male homozygous vs non carriers

C.

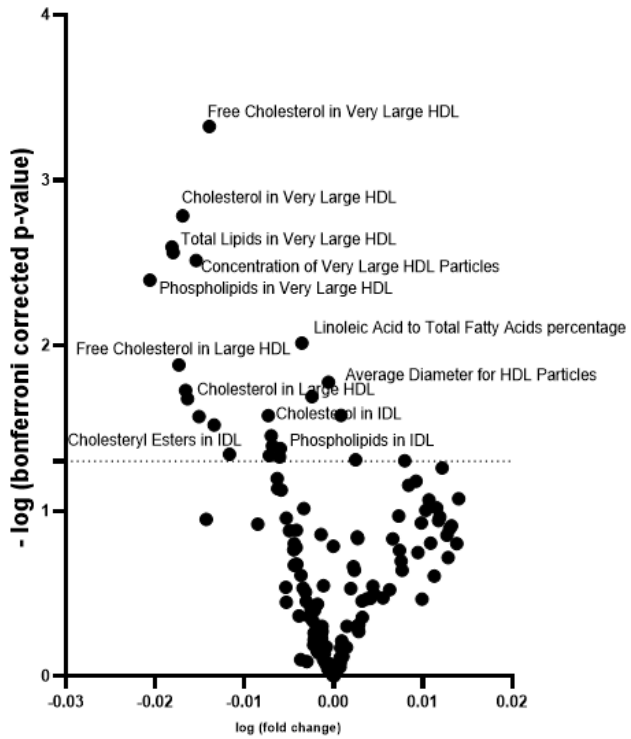

Female homozygous vs non carriers

Volcano plot for the lipidomic parameters derived from the UKB database (A), volcano plot for the lipidomic parameters in male (B), volcano plot for the lipidomic parameters in female (C). The x-axis displays the log fold change, comparison between Homozygous Pro251 carriers and non-carriers. The dotted line marks the Bonferroni significant.

Fig. S6

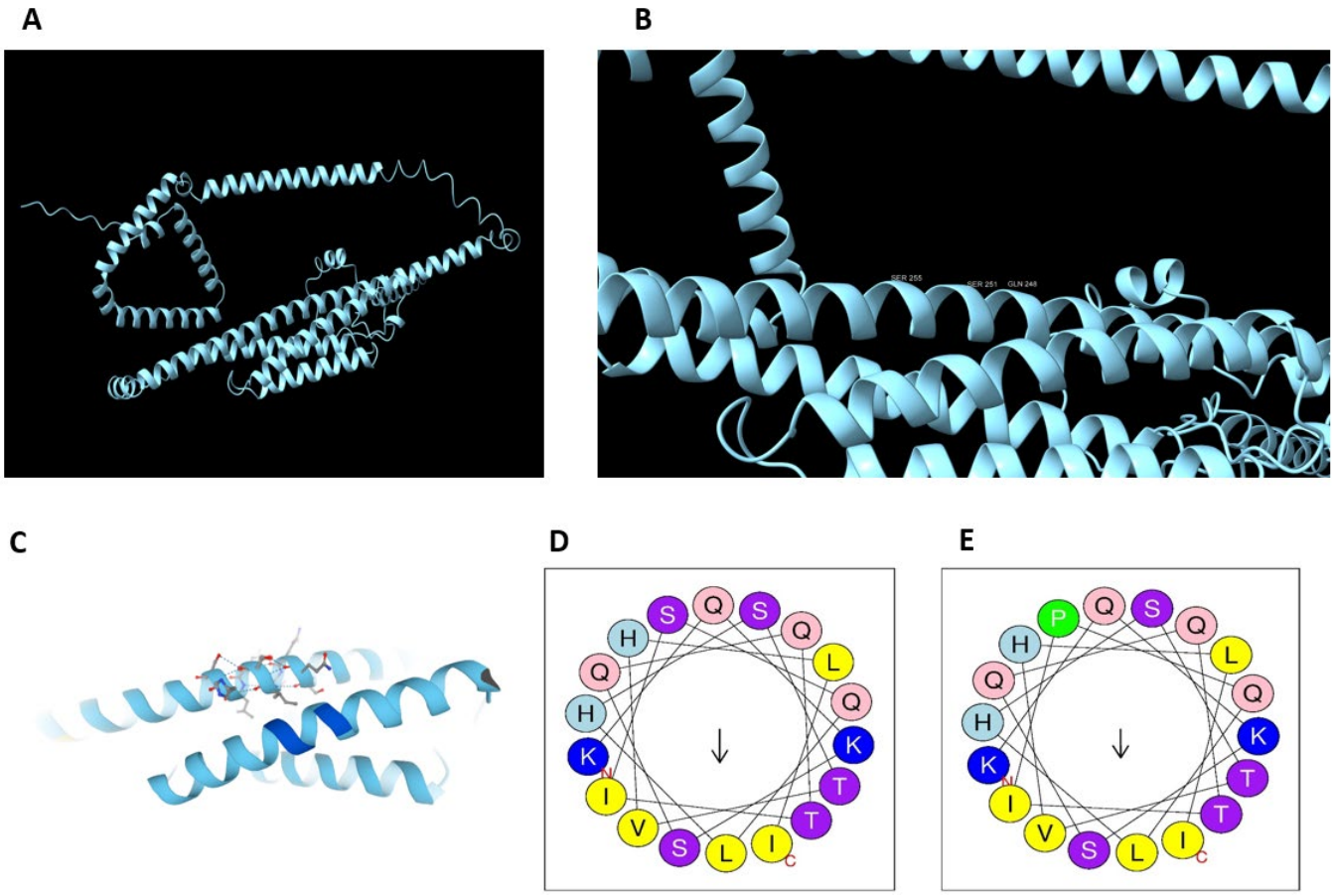

Structure of human perilipin 2 (437 amino acids) and predicted by AlphaFold (A); Expanded view of PLIN2 structure showing that S251 is situated in the 4-helix bundle domain and in the middle of a long helix that spans residues from T225 to L281 (B); Further expansion of structure to show hydrogen bonding interactions of S251 (C). Helical wheel of residues spanning from K243 (labeled with a red N) to I260 (labeled with a red C) in wild-type human PLIN2 (D); Helical wheel of residues spanning from K243 to I260 in the S251P variant of human PLIN2 (E).

Table S1

Change in mice liver triglyceride species in both chow and FFC diet groups. Comparison between *Pro251* and *Ser251*.

	Chow diet		FFC diet	
Triglycerides	**Log2 (Fold change)**	**P value**	**Log2 (Fold change)**	**P value**
TG(12:0e_6:0_20:4)	-0.4	0.252	-1.62	0.128
TG(12:1e_6:0_22:6)	-0.4	0.302	-1.43	0.155
TG(14:0_18:2_18:3)	-0.9	0.132	-1.95	0.077
TG(14:0_22:6_22:6)	-1.2	0.005	-1.03	0.085
TG(15:0_16:0_18:1)	-1.4	0.094	-1.60	0.077
TG(15:0_16:1_18:1)	-0.5	0.245	-2.14	0.056
TG(15:0_16:1_18:2)	-1.0	0.126	-2.07	0.066
TG(15:0_18:1_18:2)	-1.0	0.063	-1.91	0.109
TG(15:0_18:1_20:5)	-1.6	0.205	-2.14	0.236
TG(15:0_18:1_22:6)	-1.0	0.034	-0.90	0.205
TG(15:0_18:2_18:2)	-0.8	0.047	-1.81	0.116
TG(15:0_18:2_18:3)	-1.0	0.113	-0.89	0.608
TG(15:0_18:2_20:5)	-1.1	0.220	-2.37	0.105
TG(15:0_18:2_20:5)	-0.4	0.499	-1.55	0.222
TG(15:0_18:2_22:6)	-0.8	0.031	-1.19	0.109
TG(15:0_22:6_22:6)	-1.2	0.006	-0.83	0.202
TG(16:0_10:0_18:2)	-1.1	0.046	-1.63	0.184
TG(16:0_12:1_18:1)	-0.5	0.359	-2.29	0.056
TG(16:0_12:1_18:2)	-0.1	0.771	-1.79	0.164
TG(16:0_14:0_16:0)	-1.0	0.337	-1.94	0.066
TG(16:0_14:0_18:1)	-1.3	0.178	-1.99	0.046
TG(16:0_14:0_18:2)	-0.5	0.536	-2.20	0.072
TG(16:0_14:0_22:6)	-1.2	0.028	-1.59	0.050
TG(16:0_14:2_22:6)	-1.5	0.158	-1.99	0.096
TG(16:0_16:0_16:0)	-1.2	0.165	-1.56	0.055
TG(16:0_16:0_17:0)	-1.1	0.141	-0.78	0.213
TG(16:0_16:0_18:1)	-1.3	0.067	-1.90	0.094
TG(16:0_16:0_24:0)	-0.8	0.314	-0.39	0.415
TG(16:0_16:1_16:1)	-0.6	0.469	-2.26	0.067
TG(16:0_16:1_18:1)	-1.2	0.134	-2.11	0.149
TG(16:0_16:1_18:3)	-1.2	0.176	-1.94	0.089
TG(16:0_17:0_18:1)	-1.3	0.060	-1.42	0.120
TG(16:0_17:1_18:1)	-1.5	0.069	-1.60	0.092
TG(16:0_18:1_18:1)	-1.9	0.008	0.78	0.593

TG(16:0_18:1_18:1)	-1.2	0.033	-1.65	0.100
TG(16:0_18:1_18:1)	-0.8	0.386	1.90	0.467
TG(16:0_18:1_18:2)	-0.2	0.581	-2.88	0.301
TG(16:0_18:1_19:0)	-0.9	0.186	-1.49	0.090
TG(16:0_18:1_20:4)	-1.1	0.040	-1.13	0.051
TG(16:0_18:1_21:0)	-1.5	0.173	-1.11	0.096
TG(16:0_18:1_22:0)	-0.9	0.217	-0.83	0.227
TG(16:0_18:1_22:6)	-0.9	0.013	-1.24	0.111
TG(16:0_18:1_23:0)	-0.7	0.340	-0.63	0.287
TG(16:0_18:1_24:0)	-0.7	0.339	-0.72	0.346
TG(16:0_18:2_18:3)	0.1	0.860	-3.25	0.215
TG(16:0_18:3_22:6)	0.1	0.899	-1.91	0.055
TG(16:0_20:5_22:6)	-0.9	0.030	-1.47	0.078
TG(16:0_22:6_22:6)	-1.4	0.026	-1.16	0.103
TG(16:0_6:0_18:1)	-0.5	0.643	-1.36	0.221
TG(16:1_12:1_18:1)	-1.0	0.106	-1.87	0.113
TG(16:1_14:0_18:2)	-1.4	0.081	-2.41	0.053
TG(16:1_14:1_18:2)	-0.3	0.355	-2.20	0.059
TG(16:1_16:1_18:1)	-1.0	0.112	-1.91	0.150
TG(16:1_18:1_18:1)	-0.9	0.030	-1.65	0.065
TG(16:1_18:1_18:2)	-1.1	0.008	-1.32	0.361
TG(16:1_18:2_18:2)	2.4	0.001	-1.11	0.190
TG(16:1_18:2_18:2)	-1.3	0.027	-2.29	0.090
TG(16:1_18:2_18:3)	-0.8	0.060	-1.63	0.111
TG(16:1_18:2_18:3)	0.2	0.780	-1.53	0.225
TG(16:1_18:3_18:3)	-0.9	0.053	-4.11	0.051
TG(17:0_18:1_18:1)	-0.8	0.110	-5.65	0.137
TG(17:0_18:1_20:4)	-1.1	0.017	-1.21	0.062
TG(17:0_18:1_20:5)	-1.1	0.059	-1.62	0.083
TG(17:0_18:1_22:5)	-0.9	0.055	0.21	0.795
TG(17:0_18:1_22:6)	-0.8	0.006	0.11	0.787
TG(17:0_20:5_20:5)	-1.5	0.022	-1.36	0.071
TG(17:0_22:6_22:6)	-0.9	0.006	-2.57	0.089
TG(18:0_16:0_16:0)	-1.4	0.152	-1.32	0.046
TG(18:0_16:0_17:0)	-1.0	0.137	-0.87	0.102
TG(18:0_16:0_18:1)	-1.3	0.055	-1.48	0.076
TG(18:0_18:0_18:0)	-0.8	0.294	-0.69	0.285
TG(18:0_18:0_20:4)	-2.0	0.015	-1.09	0.059
TG(18:0_18:1_18:1)	-1.5	0.015	-1.63	0.098
TG(18:0_18:1_22:6)	-1.2	0.001	-1.13	0.173
TG(18:0_20:4_22:6)	-0.8	0.008	-0.26	0.692
TG(18:0_22:6_22:6)	-0.8	0.070	-1.46	0.004

TG(18:0_22:6_22:6)	-1.4	0.229	-0.92	0.185
TG(18:0e_12:4_12:4)	-0.1	0.763	-1.40	0.310
TG(18:1_14:0_14:0)	-1.1	0.225	-2.19	0.049
TG(18:1_17:1_18:1)	-1.2	0.015	-1.53	0.205
TG(18:1_17:1_18:2)	-1.6	0.057	-1.71	0.126
TG(18:1_17:1_22:5)	-0.5	0.491	-1.45	0.258
TG(18:1_17:1_22:6)	-2.0	0.043	-1.13	0.092
TG(18:1_18:1_18:1)	-1.5	0.008	-1.84	0.087
TG(18:1_18:1_18:1)	0.4	0.728	-2.58	0.358
TG(18:1_18:1_18:2)	-1.0	0.001	-1.62	0.164
TG(18:1_18:1_18:2)	-0.9	0.361	-3.10	0.300
TG(18:1_18:1_18:3)	-0.9	0.003	-1.50	0.229
TG(18:1_18:1_20:3)	-0.9	0.004	-0.77	0.330
TG(18:1_18:1_20:3)	-1.5	0.035	-1.36	0.053
TG(18:1_18:1_20:4)	-1.1	0.025	-1.76	0.071
TG(18:1_18:1_20:4)	-1.9	0.074	-1.11	0.254
TG(18:1_18:1_20:5)	-1.0	0.009	-1.37	0.138
TG(18:1_18:1_21:0)	-1.1	0.124	-0.72	0.347
TG(18:1_18:1_21:1)	-1.2	0.051	-1.71	0.059
TG(18:1_18:1_22:0)	-1.5	0.078	-1.04	0.225
TG(18:1_18:1_22:1)	-1.6	0.148	-1.37	0.117
TG(18:1_18:1_22:3)	0.1	0.785	-1.61	0.001
TG(18:1_18:1_22:4)	-1.2	0.008	-1.34	0.065
TG(18:1_18:1_22:5)	-1.4	0.008	-1.51	0.106
TG(18:1_18:1_22:6)	-1.9	0.036	-1.16	0.221
TG(18:1_18:1_23:0)	-0.8	0.273	-0.44	0.450
TG(18:1_18:1_23:1)	-0.7	0.455	-0.92	0.232
TG(18:1_18:1_24:1)	-1.6	0.050	-1.23	0.217
TG(18:1_18:2_18:3)	-0.5	0.412	-1.04	0.197
TG(18:1_18:2_20:4)	-1.0	0.008	-1.61	0.171
TG(18:1_18:2_20:4)	0.1	0.828	-1.30	0.118
TG(18:1_18:2_20:5)	-0.4	0.431	-1.13	0.191
TG(18:1_18:2_21:1)	-1.3	0.012	-1.59	0.111
TG(18:1_18:2_22:1)	-1.6	0.024	-1.72	0.141
TG(18:1_18:2_22:5)	-1.5	0.000	-1.04	0.130
TG(18:1_18:2_22:6)	-1.0	0.001	-1.26	0.156
TG(18:1_18:2_24:1)	-1.2	0.058	-1.07	0.249
TG(18:1_20:3_22:6)	-1.2	0.019	-1.22	0.079
TG(18:1_20:4_22:6)	-1.3	0.002	-0.78	0.171
TG(18:1_20:5_22:6)	-1.1	0.013	-0.85	0.205
TG(18:1_22:0_22:6)	-0.8	0.157	0.80	0.359
TG(18:1_22:1_22:6)	-1.4	0.024	0.90	0.464

TG(18:1_22:5_22:5)	-0.7	0.363	-0.92	0.060
TG(18:1_22:5_22:6)	-1.4	0.006	-0.31	0.629
TG(18:1_22:6_22:6)	-1.2	0.001	-0.78	0.223
TG(18:2_17:1_18:2)	-0.9	0.033	-1.64	0.151
TG(18:2_17:1_18:2)	0.9	0.327	-1.66	0.016
TG(18:2_17:1_20:4)	-0.9	0.072	-1.88	0.110
TG(18:2_17:1_22:6)	-0.9	0.033	-1.22	0.119
TG(18:2_18:2_18:2)	-1.1	0.000	-1.81	0.219
TG(18:2_18:2_20:4)	-0.8	0.007	-1.08	0.172
TG(18:2_18:2_22:6)	-1.0	0.002	-1.19	0.067
TG(18:2_18:2_22:6)	-0.9	0.007	-1.05	0.256
TG(18:2_22:6_22:6)	-1.0	0.014	-0.71	0.347
TG(18:2_22:6_22:6)	-0.8	0.143	-0.67	0.536
TG(18:2+5O_16:0_16:0)	-0.7	0.008	-1.98	0.103
TG(18:3_17:1_18:2)	-0.9	0.154	-1.48	0.094
TG(18:3_18:2_18:2)	-1.2	0.161	-3.45	0.324
TG(18:3_18:2_18:2)	0.5	0.455	-2.06	0.241
TG(18:3_18:2_18:3)	-0.7	0.036	-1.50	0.276
TG(18:3_18:2_18:3)	-0.3	0.593	-2.34	0.074
TG(18:3_18:2_20:5)	-0.7	0.046	-1.49	0.140
TG(18:3_18:2_22:6)	-0.6	0.042	-1.38	0.192
TG(18:3_18:3_18:3)	-0.5	0.381	-1.47	0.114
TG(18:3_22:6_22:6)	-0.8	0.018	-0.58	0.396
TG(18:3+5O_16:0_16:0)	-0.7	0.011	-1.82	0.203
TG(18:4_16:1_16:1)	-0.9	0.188	-1.97	0.066
TG(18:4_16:1_18:2)	-0.2	0.818	-1.37	0.080
TG(18:4_18:1_18:1)	-1.2	0.006	-1.41	0.096
TG(19:0_18:1_18:1)	-1.3	0.057	-1.29	0.110
TG(19:0_18:1_20:4)	-1.0	0.025	-0.20	0.710
TG(19:1_16:0_18:1)	-1.5	0.037	-1.37	0.102
TG(19:1_18:1_18:1)	-2.4	0.083	-1.55	0.089
TG(19:1_18:1_18:2)	-1.2	0.004	-1.49	0.110
TG(19:1_18:2_18:2)	-1.0	0.185	-1.68	0.113
TG(19:1_18:2_22:6)	-1.4	0.004	-0.82	0.319
TG(19:1_20:5_20:5)	-1.5	0.029	-1.01	0.168
TG(20:0_16:0_16:0)	-1.2	0.196	-0.75	0.140
TG(20:0_16:0_18:1)	-1.2	0.159	-1.29	0.136
TG(20:0_18:1_18:1)	-1.7	0.031	-1.32	0.140
TG(20:0_18:1_22:6)	-1.0	0.021	-0.74	0.344
TG(20:1_18:1_18:1)	-3.6	0.004	-1.70	0.098
TG(20:1_18:1_18:1)	-0.7	0.124	1.57	0.099
TG(20:1_18:1_18:2)	-1.0	0.003	-0.20	0.875

TG(20:1_18:1_18:2)	-1.1	0.004	-1.63	0.137
TG(20:1_18:1_18:2)	-1.0	0.028	-1.36	0.107
TG(20:1_18:1_22:5)	-1.2	0.009	-1.29	0.090
TG(20:1_18:2_22:6)	-1.4	0.061	-1.17	0.067
TG(20:3_18:2_22:6)	-1.4	0.002	-1.18	0.164
TG(20:4e_18:1_18:1)	0.7	0.120	-1.26	0.245
TG(20:5_17:1_18:2)	-2.0	0.017	-1.47	0.007
TG(20:5_18:2_18:2)	-0.9	0.023	-1.49	0.130
TG(20:5_18:2_20:5)	-0.5	0.254	-1.50	0.252
TG(20:5_18:2_22:5)	-0.9	0.014	-1.29	0.206
TG(20:5_18:2_22:6)	-0.5	0.183	-1.25	0.257
TG(22:1_18:2_22:6)	-0.3	0.518	1.58	0.050
TG(22:5_17:1_18:2)	-1.1	0.004	-2.00	0.117
TG(22:5_18:2_18:2)	-1.3	0.001	-0.92	0.184
TG(22:5_18:2_22:6)	-1.2	0.001	-1.01	0.381
TG(22:6_17:1_22:6)	-0.9	0.005	-2.65	0.337
TG(22:6_17:1_22:6)	-0.9	0.073	-0.77	0.486
TG(24:0_18:2_18:2)	-0.3	0.448	-0.35	0.563
TG(28:0_10:4_18:2)	-0.5	0.117	-1.95	0.200
TG(30:0_18:1_18:1)	-1.6	0.184	-0.51	0.521
TG(4:0_16:0_16:0)	-1.1	0.380	-0.68	0.505
TG(4:0_16:0_18:1)	-1.0	0.439	-0.55	0.628
TG(4:0_16:0_18:2)	-0.9	0.441	-0.64	0.684
TG(4:0_18:1_18:2)	-1.2	0.378	-0.88	0.464

Log2 fold change for each triglyceride (TG). Bonferroni corrected/adjusted p value, by dividing the original α-value (0.05) by the number of analyses on the dependent variable.

Table S2

***PLIN2 rs35568725* prevalence in the MVP population (Caucasic, African American, Hispanic)**

Population	Reference	Alternative	MAF	Phenotype	Beta	SE	P
Trans-ethnic	A	G	0.051	ALT	0.005	0.003	0.142
White	A	G	0.055	ALT	0.004	0.003	0.250
Black	A	G	0.013	ALT	0.014	0.013	0.276
Hispanic	A	G	0.028	ALT	0.006	0.015	0.690
Asians	A	G	0.020	ALT	0.031	0.052	0.559
Trans-ethnic	A	G	0.052	NAFLD	0.021	0.015	0.160

White	A	G	0.055	NAFLD	0.031	0.016	0.051
Black	A	G	0.013	NAFLD	-0.068	0.070	0.330
Hispanic	A	G	0.029	NAFLD	-0.089	0.070	0.203
Asians	A	G	0.022	NAFLD	0.120	0.226	0.597

Additive logistic model corrected for age, sex, and the first ten ethnicity-specific principal components.

Table S3

Association between PLIN2-Pro251 and type 2 diabetes, dyslipidemia, hypertension, and NAFLD in the MVP database (before Bonferroni correction)

Phenotype	Beta	SE	P	OR	95% Low	95% High
NAFLD	0.003	0.003	0.25	1.00	0.99	1.01
T2D	0.06	0.02	0.002	1.07	1.02	1.11
Cardiomyopathy	0.07	0.03	0.016	1.08	1.01	1.15

Multivariable analysis adjusted for age, gender, and 5 PC principal components European Ancestry

Table S4

Hepatic liver fat after adjustment for visceral adipose tissue:

Phenotype	Beta	SE	P-value
Liver volume	-2.812e-03	3.667e-03	0.443
MRI-PDFF	-0.0973086	0.0732235	0.183
Liver iron	1.505257	0.866653	0.082

Multivariable analyses adjusted for age, sex, BMI, visceral adipose tissue, and PC1-10.

Table S5

Magnetic resonance imaging-derived proton density fat fraction (MRI-PDFF) in BMI categories:

BMI: <18.5

Phenotype	Beta	SE	P-value
MRI-PDFF	0.334	0.186	0.075
Visceral adipose tissue	-0.007	0.160	0.962

Multivariable analyses adjusted for age, sex, and PC1-10.

BMI: from 18.5 to 25

Phenotype	Beta	SE	P-value
MRI-PDFF	0.032	0.067	0.630
Visceral adipose tissue	-6.542e-17	2.791e-16	0.814

Multivariable analyses adjusted for age, sex, and PC1-10.

BMI: from 25 to 30

Phenotype	Beta	SE	P-value
MRI-PDFF	-0.212	0.118	0.071
Visceral adipose tissue	1.840e-16	1.286e-16	0.152

Multivariable analyses adjusted for age, sex, and PC1-10.

BMI: >30

Phenotype	Beta	SE	P-value
MRI-PDFF	-0.203	0.255	0.425
Visceral adipose tissue	-1.494e-16	1.432e-16	0.296

Multivariable analyses adjusted for age, sex, and PC1-10.

Supplementary reference

1. Carr RM, Peralta G, Yin X, Ahima RS. Absence of perilipin 2 prevents hepatic steatosis, glucose intolerance and ceramide accumulation in alcohol-fed mice. PloS one. 2014;9(5):e97118.